Chapter 5

A Model of Tumour Angiogenesis and Anti-Angiogenic Strategies

In this chapter, we apply the modelling approach developed in chapter 4 to an *in vivo* scenario of tumour-induced angiogenesis. The work is based on the continuous model of Levine *et al.* [87] (see also section 2.5.1) and consists of two coupled systems: a one-dimensional system, representing a capillary, and a two-dimensional system, representing the ECM which separates the capillary from the tumour. In the capillary, the EC respond to a VEGF stimulus by producing protease, which degrades the basement membrane and eventually allows the EC to move into the ECM. Once in the ECM, the cells can migrate towards the tumour, continuing to secrete protease and thus degrading the ECM. The protease is viewed as a chemoattractant, whilst haptotaxis is assumed to have the effect of attracting the EC to areas where the density of the ECM is low. In line with experimental observations, EC proliferation is included in the ECM. The capillary and the ECM are coupled via appropriate transmission conditions. The model thus incorporates the initial stages of angiogenesis, in which the EC must abandon their normally quiescent state and move out of the parent capillary, a feature often neglected in other models.

The effects of angiostatin, an angiogenic inhibitor (see section 1.5.6), are also examined. Angiostatin is assumed to function by deactivating the protease produced by the EC [153], either directly or indirectly via an intermediate, EC-derived inhibitor

complex.

We formulate this scenario as a reinforced random walk model. Section 5.1 contains the details of the mathematical model, which describes how the substrate concentrations evolve in space and time, how the EC move and how the capillary and ECM are coupled. In section 5.2, the method of simulation is described, including details of how cell proliferation and death take place and how these affect the observable formation of new capillaries. The model parameters are discussed in section 5.3. The results are presented in section 5.4 and discussed in section 5.5.

5.1 The Mathematical Model

The model is constructed on the domain shown in Figure 5.1 and on the time domain, $[0, T]$. The parent capillary is assumed to be of infinitesimal thickness, and is located on the subset of the x-axis, $[0, L]$. The ECM separating the capillary and the tumour is viewed as the rectangular subset of the xy–plane, $[0, L] \times [0, l]$. Functions defined on the capillary will be denoted by lower-case letters, $g : [0, L] \times [0, T] \to \mathbb{R}$, whereas functions defined on the ECM will be denoted by upper-case letters, $G : [0, L] \times [0, l] \times [0, T] \to \mathbb{R}$. We distinguish between quantities in the capillary and quantities just outside the capillary: in general, $g(x, t) \neq G(x, 0, t)$. This was the setup used in [87].

We begin with a number of EC in the parent capillary and a source of VEGF at the tumour. We model the concentration of fibronectin, a principal component of the ECM, in the capillary and the ECM. Thus fibronectin concentration is viewed as representing the thickness of the basement membrane in the parent capillary, and the density of the ECM. The VEGF diffuses through the ECM and into the capillary, where it binds to receptors on the surface of EC. This stimulates the EC to produce a protease, which in turn degrades the fibronectin levels in the capillary. The Michaelis–Menten hypothesis will be used for these biochemical reactions.

When the fibronectin concentration in the capillary falls below a certain threshold level, the basement membrane has been sufficiently degraded to allow EC to escape into the ECM. The EC continue to produce protease in the ECM and can thus degrade fibronectin levels there. EC movement is governed by both random diffusion and by chemotactic and haptotactic terms. We assume, as discussed in section

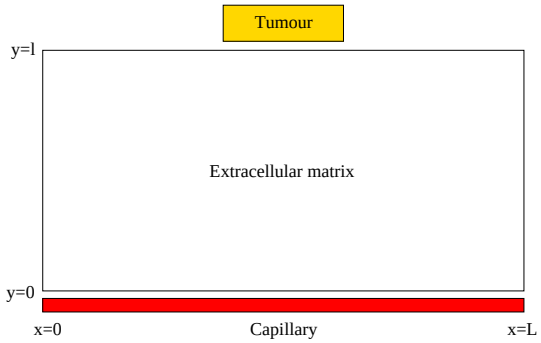

Figure 5.1: A diagram of the model geometry.

5.1.2, that VEGF and protease are chemoattractants for the EC, whilst haptotaxis has the effect of attracting cells to regions of low fibronectin concentration. EC proliferation in the ECM is comprised of a background growth term and a protease-dependent term, so the amount of protease produced by the EC in turn affects the EC proliferation response. A death term is also included, representing apoptosis, or programmed cell death [94]. We expect the EC to form sprouts from the capillary and migrate across the ECM towards the tumour.

Angiostatin, an anti-angiogenic factor, is assumed to function by directly inhibiting the actions of the protease. We will investigate whether this mechanism can curtail angiogenic activity.

5.1.1 The Substrate Dynamics

As in [90], we take the view that the binding of ligand to cell receptors can be modelled as an enzymatic biochemical reaction (see also [74]). The reaction of particular interest here is the binding of VEGF to receptors located on EC. A molecule of VEGF (V) binds to a receptor on the surface of an EC (R_V), forming a receptor–ligand complex ($R_V V$). The complex is internalised and triggers an intracellular sequence of transcription events, the result of which is the secretion of a number of molecules of protease (C). The complex decomposes into a modified receptor (R'_V), which is subsequently recycled back to the cell surface to become R_V, where it may repeat the process. There is hence an uptake of VEGF by EC [82], stimulating expression of protease [118].

The transduction cascade triggered by the binding of VEGF is highly complex

and involves G-proteins, amplification events and mRNA [91]. The process is not fully understood and many of the individual rate constants are unknown. Here we consider a simplified mechanism, which does not take account of intracellular events, but retains the most important biochemical features. This may be written symbolically as follows:

$$V + R_V \underset{k_{-1}}{\overset{k_1}{\rightleftharpoons}} R_V V,$$

$$R_V V \xrightarrow{k_2} C + R_V.$$

Denoting the concentration of a substance X by $[X]$, we apply to this process the law of mass action (see section 2.1.1). Let $[R_T]$ be the total receptor concentration (free receptors plus receptors forming the intermediate complex). In addition to the changes in the concentrations of the individual species resulting from the above reaction, $[R_T]$ may change with time due to, for example, local crowding or dispersion of cells. Taking this into account, we therefore have the following set of equations:

$$\frac{d[R_V]}{dt} = -k_1[R_V][V] + (k_{-1} + k_2)[R_V V] + \frac{d[R_T]}{dt}, \tag{5.1}$$

$$\frac{d[V]}{dt} = -k_1[R_V][V] + k_{-1}[R_V V], \tag{5.2}$$

$$\frac{d[R_V V]}{dt} = k_1[R_V][V] - (k_{-1} + k_2)[R_V V], \tag{5.3}$$

$$\frac{d[C]}{dt} = k_2[R_V V]. \tag{5.4}$$

We proceed as in section 2.1.3. It is assumed, as in [90], that the total number of receptors per cell is a constant, $\delta_e > 0$. We thus replace $[R_T]$ by $\delta_e[EC]$, where $[EC]$ is the endothelial cell density. This yields the following pair of rate laws for the VEGF and protease:

$$\frac{d[V]}{dt} = -\frac{\lambda_1 \delta_e [V][EC]}{1 + \nu_1[V]}, \tag{5.5}$$

$$\frac{d[C]}{dt} = \frac{\lambda_1 \delta_e [V][EC]}{1 + \nu_1[V]}, \tag{5.6}$$

where $\nu_1 = \frac{k_1}{k_{-1}+k_2}$, $\lambda_1 = \nu_1 k_2$. The dynamics for $[EC]$ will be considered in section 5.1.2.

Degradation of fibronectin (F) by protease can also be viewed as an enzymatic reaction. In addition, angiostatin acts by inhibiting the protease [153]. We therefore assume that the total protease (C) consists of a proportion that is active (C_A), a proportion that is inactive (C_I), as well as a proportion that is in the intermediate

complex (C_AF). Angiostatin (A) combines with active protease to form inactive protease, which is inhibited from functioning in the degradation of fibronectin. These reactions are written:

$$C_A + F \underset{k_{-5}}{\overset{k_5}{\rightleftharpoons}} C_AF,$$

$$C_AF \xrightarrow{k_6} C_A + F',$$

$$A + C_A \underset{k_{-7}}{\overset{k_7}{\rightleftharpoons}} C_I,$$

where F' represents proteolytic fragments of fibronectin.

Again, in addition to the changes in the individual species concentrations caused by these reactions, the total protease concentration will change with time. The protease secreted by the cells is initially in the active form, so (5.6) provides a contribution to $\frac{d[C_A]}{dt}$[1]. Hence the law of mass action yields the following set of equations:

$$\begin{aligned}
\frac{d[C_A]}{dt} &= -k_5[C_A][F] + (k_{-5}+k_6)[C_AF] - k_7[C_A][A] + k_{-7}[C_I] + \frac{d[C]}{dt}, \\
\frac{d[F]}{dt} &= -k_5[C_A][F] + k_{-5}[C_AF], \\
\frac{d[C_AF]}{dt} &= k_5[C_A][F] - (k_{-5}+k_6)[C_AF], \\
\frac{d[F']}{dt} &= k_6[C_AF], \\
\frac{d[A]}{dt} &= -k_7[C_A][A] + k_{-7}[C_I], \\
\frac{d[C_I]}{dt} &= k_7[C_A][A] - k_{-7}[C_I].
\end{aligned}$$

If $[C_AF](0) = [C_I](0) = [F'](0) = 0$, then it follows that

$$\begin{aligned}
[C_A] + [C_AF] + [C_I] &= [C], \\
[F] + [C_AF] + [F'] &= [F](0).
\end{aligned}$$

Assuming that the angiostatin reaction is in equilibrium, we have $[C_I] = \nu_e[C_A][A]$ (where $\nu_e = \frac{k_7}{k_{-7}}$) and hence

$$[C_A] = \frac{[C] - [C_AF]}{1 + \nu_e[A]}.$$

[1] *In vivo*, there may be additional contributions from other sources. For example, tissue plasminogen activators, which may be expressed by activated EC and by tumour cells [122], convert the inert substance plasminogen into plasmin, which is a proteolytic enzyme.

A similar application of the Michaelis–Menten hypothesis determines $[C_A F]$ and leads to the rate law for fibronectin,

$$\frac{d[F]}{dt} = -\lambda_3 [C_A][F],$$

where

$$[C_A] = \frac{[C]}{1 + \nu_e [A] + \nu_3 [F]},$$

and $\nu_3 = \frac{k_5}{k_{-5}+k_6}$, $\lambda_3 = \nu_3 k_6$.

Now let $v(x,t)$, $c(x,t)$, $f(x,t)$ and $a(x,t)$ respectively denote the concentrations of VEGF, (total) protease, fibronectin and angiostatin in the capillary. Also let $p(x,t)$ denote the EC density. We now combine the reaction kinetics described above with:

- A source term, $v_r(x,t)$, allowing VEGF to pass into the capillary from the ECM.
- Natural decay of protease (with rate constant, $\mu \geq 0$).
- Logistic production of fibronectin by the EC (with carrying capacity, $f_0 > 0$)[2].
- A source of angiostatin, $a_r(x,t)$, and natural decay of angiostatin (with characteristic decay time, $T_a > 0$).

This leads to the following system of differential equations:

$$\frac{\partial v}{\partial t} = -\frac{\lambda_1 \delta_e v p}{1 + \nu_1 v} + v_r(x,t), \tag{5.7}$$

$$\frac{\partial c}{\partial t} = \frac{\lambda_1 \delta_e v p}{1 + \nu_1 v} - \mu c, \tag{5.8}$$

$$\frac{\partial f}{\partial t} = \frac{4}{T_f} f \left(1 - \frac{f}{f_0}\right) \frac{p}{p_0} - \lambda_3 c_a f, \tag{5.9}$$

$$\frac{\partial a}{\partial t} = a_r(x,t) - \frac{a}{T_a}. \tag{5.10}$$

Note that only the active protease, c_a, takes part in the degradation of fibronectin, and we have

$$c_a = \frac{c}{1 + \nu_e a + \nu_3 f}. \tag{5.11}$$

[2]EC exhibit a strong tendency to secrete ECM components, such as fibronectin [17, 36]. Note, however, that no secretion will take place until proteolysis has reduced the fibronectin concentration below its initial level of f_0. Only once the EC have been activated, and angiogenesis is underway, will fibronectin secretion begin [35].

Diffusion has been neglected here as it takes place on a much longer time scale than the kinetic reactions in the capillary. However it is necessary to include diffusion terms for the VEGF, fibronectin and angiostatin in the ECM.

Although EC will continue to secrete fibronectin in the ECM, there will also be fibronectin synthesis by cells residing throughout the ECM, primarily fibroblasts [35]. We therefore use a logistic growth law that is independent of P for fibronectin synthesis in the ECM.

The exogenously supplied angiostatin, in addition to being delivered to the parent capillary, will be delivered to the new capillaries. The trajectories of the new capillaries will correspond to areas where the ECM has been degraded by the migrating EC [122]. We therefore include an angiostatin source term, $a_r(x,t)\left(1-\frac{F}{f_0}\right)$ [87].

Thus we have the following system of PDEs in the ECM[3]:

$$\frac{\partial V}{\partial t} = D_V\nabla^2 V - \frac{\lambda_1\delta_e VP}{1+\nu_1 V}, \tag{5.12}$$

$$\frac{\partial C}{\partial t} = \frac{\lambda_1\delta_e VP}{1+\nu_1 V} - \mu C, \tag{5.13}$$

$$\frac{\partial F}{\partial t} = D_F\nabla^2 F + \frac{4}{T_F}F\left(1-\frac{F}{f_0}\right) - \lambda_3 C_A F, \tag{5.14}$$

$$\frac{\partial A}{\partial t} = D_A\nabla^2 A + a_r(x,t)\left(1-\frac{F}{f_0}\right) - \frac{A}{T_a}, \tag{5.15}$$

where $D_V, D_F, D_A, T_F > 0$ are constants.

The active protease law also applies in the ECM:

$$C_A = \frac{C}{1+\nu_e A+\nu_3 F}. \tag{5.16}$$

[3]The sink term in equation (5.12) represents uptake and binding of VEGF by the actively migrating EC in the ECM, whereas the corresponding term in equation (5.7) represents uptake and binding of VEGF by EC in the parent vessel. We emphasise this distinction since the parent capillary is regarded as a mature vessel with a well defined barrier (the basement membrane) which chemical species must cross in order to enter or leave the circulation, whereas in the ECM, the migrating EC have an immature phenotype and there is no basement membrane separating them from diffusing proteins. VEGF may therefore be bound directly by EC in the ECM, via the uptake term in (5.12), but must first cross the capillary wall (see boundary condition (5.29) below) before it may be bound by EC in the parent vessel, via (5.7).

5.1.2 The Endothelial Cell Dynamics

In the quiescent endothelium, connections between neighbouring EC are tight and there is little or no cell movement [55]. However, during angiogenesis, cell–cell connections are loosened and EC migrate towards the tumour [120]. It is therefore important to account for EC movement, which we do using the reinforced random walk theory described in chapter 3.

We assume that the EC of the parent capillary move on a regular mesh of size h. Let $p_n(t)$ be the EC density at mesh point n at time t. We use the one-dimensional master equation (3.4):

$$\frac{\partial p_n}{\partial t} = \hat{\tau}^+_{n-1} p_{n-1} + \hat{\tau}^-_{n+1} p_{n+1} - \left(\hat{\tau}^+_n + \hat{\tau}^-_n\right) p_n, \tag{5.17}$$

with the standard normalised transition probabilities (3.8):

$$\hat{\tau}^{\pm}_n = \frac{2\lambda\tau\left(w_{n\pm\frac{1}{2}}\right)}{\tau\left(w_{n-\frac{1}{2}}\right) + \tau\left(w_{n+\frac{1}{2}}\right)}, \tag{5.18}$$

where $\lambda h^2 = D_p \geq 0$ and w is the vector of control substances.

Levine *et al.* [87] took $\tau = \tau(c_a, f)$ and did not include any dependence on VEGF. However, the exact roles of the various control substances are not fully understood and the appropriate form for τ is unclear. In an attempt to investigate the functions of the control substances, we take $\tau = \tau(c_a, f, v)$ and look at various possibilities for the exact form of τ.

VEGF is a potent chemoattractant for EC [77], so EC will migrate towards regions of high VEGF concentration. Similarly, protease will be expressed, in response to VEGF, in areas of angiogenic activity, so we assume that protease also has a chemotactic effect on the EC.

The effect of ECM components, such as fibronectin, on the directional movement of cells is unclear and there is conflicting experimental evidence. Some authors have reported migration of cells up fibronectin concentration gradients [21]. However, others have suggested that proteolytic fragments of fibronectin may act as chemoattractants for EC, which will consequently migrate to areas of tissue degradation, where the fibronectin concentration is low [110]. Furthermore, undegraded extracellular tissue represents a significant barrier to cell movement *in vivo* and,

during angiogenesis, EC secrete proteolytic enzymes to degrade the ECM, facilitating migration [122, 124]. Taking fibronectin concentration as a measure of the penetrability of the tissue, we therefore take the view that EC are attracted to regions of *low* fibronectin. They will thus move towards areas where the ECM has been degraded, and where they can hence move more freely.

Hence $\tau(c_a, f, v)$ should be an increasing function of c_a and v and a decreasing function of f. In order to avoid singularities in $\ln\tau$ and its derivatives, we take

$$\tau(c_a, f, v) = \left(\frac{c_a+\alpha_1}{c_a+\alpha_2}\right)^{\gamma_1}\left(\frac{f+\beta_1}{f+\beta_2}\right)^{\gamma_2}\left(\frac{v+\delta_1}{v+\delta_2}\right)^{\gamma_3}, \tag{5.19}$$

where $0<\alpha_1,\delta_1<\alpha_2,\delta_2$, $0<\beta_2<\beta_1$ and $\gamma_1,\gamma_2,\gamma_3>0$.

The chemotactic sensitivity associated with this choice is

$$\frac{\tau_x}{\tau} = \gamma_1\frac{\alpha_2-\alpha_1}{(c_a+\alpha_1)(c_a+\alpha_2)}\frac{\partial c_a}{\partial x} + \gamma_2\frac{\beta_2-\beta_1}{(f+\beta_1)(f+\beta_2)}\frac{\partial f}{\partial x} + \gamma_3\frac{\delta_2-\delta_1}{(v+\delta_1)(v+\delta_2)}\frac{\partial v}{\partial x},$$

which reflects the fact that cells become desensitised to chemotactic gradients when the concentration of the control substance is high [4].

The two-dimensional version of the master equation (3.10), governing cell movement in the ECM is:

$$\begin{aligned}\frac{\partial P_{n,m}}{\partial t} &= \hat{T}^{H+}_{n-1,m}P_{n-1,m} + \hat{T}^{H-}_{n+1,m}P_{n+1,m} + \hat{T}^{V+}_{n,m-1}P_{n,m-1} + \hat{T}^{V-}_{n,m+1}P_{n,m+1} \\ &\quad - \left(\hat{T}^{H+}_{n,m} + \hat{T}^{H-}_{n,m} + \hat{T}^{V+}_{n,m} + \hat{T}^{V-}_{n,m}\right)P_{n,m},\end{aligned} \tag{5.20}$$

where

$$\hat{T}^{H\pm}_{n,m} = \frac{4\lambda T\left(W_{n\pm\frac{1}{2},m}\right)}{T\left(W_{n-\frac{1}{2},m}\right)+T\left(W_{n+\frac{1}{2},m}\right)+T\left(W_{n,m-\frac{1}{2}}\right)+T\left(W_{n,m+\frac{1}{2}}\right)}, \tag{5.21}$$

$$\hat{T}^{V\pm}_{n,m} = \frac{4\lambda T\left(W_{n,m\pm\frac{1}{2}}\right)}{T\left(W_{n-\frac{1}{2},m}\right)+T\left(W_{n+\frac{1}{2},m}\right)+T\left(W_{n,m-\frac{1}{2}}\right)+T\left(W_{n,m+\frac{1}{2}}\right)}, \tag{5.22}$$

and the superscripts, H and V, denote movement in the horizontal and vertical directions respectively.

In addition to migration, EC proliferation is an important component of angiogenesis [120]. We therefore add a proliferation term, Γ, to the master equation (5.20):

$$\Gamma = P\left[\left(Q + G(C_A)\frac{\partial C_A}{\partial t}\right) - \mu_1\right], \tag{5.23}$$

where $Q, \mu_1 \geq 0$ are constants. The method used to incorporate this term into simulations based on the master equation (5.20) will be discussed in section 5.2.

The first term inside the square brackets represents EC proliferation; the second represents natural death by apoptosis. The QP term represents a constant (low) level of background proliferation, whilst the $G(C_A)$ term represents a protease-dependent contribution to cell proliferation. Proteolytic enzymes have two opposing effects on EC [87]: low concentrations of protease are observed to stimulate proliferation [30]; high concentrations result in cell disintegration and death. Thus the proliferation response fraction, $\Theta \equiv \frac{P(t)-P(0)}{P(0)}$, will initially increase with active protease, but will subsequently fall off to zero as the active protease concentration becomes high [166]. We therefore choose

$$\Theta = AC_A \exp\left(-\lambda_0 C_A^{m_1}\right),$$

where $A, \lambda_0, m_1 > 0$ are constants.

Note that one can write $P(t) = P(0)(1+\Theta)$, so $P'(t) = P(0)\Theta' \frac{\partial C_A}{\partial t}$. Eliminating $P(0)$ yields $P'(t) = P\frac{\Theta'}{1+\Theta}\frac{\partial C_A}{\partial t}$. We therefore choose

$$G(C_A) = \frac{\Theta'(C_A)}{1+\Theta(C_A)} = \frac{A\exp\left(-\lambda_0 C_A^{m_1}\right)\left(1-\lambda_0 m_1 C_A^{m_1}\right)}{1+AC_A\exp\left(-\lambda_0 C_A^{m_1}\right)}. \tag{5.24}$$

We take $T(C_A, F, V)$ to be of the same form as (5.19):

$$T(C_A, F, V) = \left(\frac{C_A+\alpha_3}{C_A+\alpha_4}\right)^{\gamma_4}\left(\frac{F+\beta_3}{F+\beta_4}\right)^{\gamma_5}\left(\frac{V+\delta_3}{V+\delta_4}\right)^{\gamma_6}, \tag{5.25}$$

where $0 < \alpha_3, \delta_3 < \alpha_4, \delta_4$, $0 < \beta_4 < \beta_3$ and $\gamma_4, \gamma_5, \gamma_6 > 0$.

We use the master equations (5.17) and (5.20), along with rules for branching and looping (see section 5.2), to simulate the behaviour of individual EC in the capillary and the ECM respectively.

5.1.3 Initial, Boundary and Transmission Conditions

For the model to function as required, the ECM and capillary equations must be coupled by appropriate transmission conditions. The rate of supply of VEGF to the capillary, $v_r(x,t)$, is assumed to depend on the difference between the VEGF concentration just outside the capillary wall, $V(x,0,t)$, and in the capillary, $v(x,t)$

[87]:

$$v_r(x,t) = B_1\left(V(x,0,t) - v(x,t)\right), \tag{5.26}$$

for $B_1 \geq 0$ constant.

Angiostatin is supplied intravenously, at a constant rate, $A_r \geq 0$, after an initial period, $T_{\text{iv}} \geq 0$:

$$a_r(x,t) = A_r H\left(t - T_{\text{iv}}\right). \tag{5.27}$$

Furthermore, it is assumed that EC cannot move into the ECM until the fibronectin concentration in the capillary falls below a certain threshold level, f_1. The fibronectin concentration in the capillary, $f(x,t)$, is viewed as a measure of the penetrability of the basement membrane: a high concentration corresponding to an intact and impenetrable membrane; a low concentration corresponding to a degraded membrane. The EC must proteolytically degrade the basement membrane before they can escape from the parent vessel into the ECM [121]. We therefore assume that an EC can only move from the capillary to the ECM once the local fibronectin concentration has fallen below the threshold level, f_1. This may be written mathematically:

$$P(x,0,t) = H\left(f_1 - f(x,t)\right) p(x,t). \tag{5.28}$$

We need boundary conditions for the VEGF, fibronectin and angiostatin. Across the interface between the capillary and the ECM, we assume that there is no flux of fibronectin, and that the flux of VEGF and angiostatin is proportional to the difference between the concentrations in the capillary and in the ECM. Boundary conditions at the capillary side of the ECM are therefore taken as follows[4]:

$$-D_V \frac{\partial V(x,0,t)}{\partial y} + \psi\left(V(x,0,t) - v(x,t)\right) = 0, \tag{5.29}$$

$$-D_F \frac{\partial F(x,0,t)}{\partial y} = 0, \tag{5.30}$$

$$-D_A \frac{\partial A(x,0,t)}{\partial y} + \psi'\left(A(x,0,t) - a(x,t)\right) = 0, \tag{5.31}$$

for constants $\psi, \psi' \geq 0$.

[4]One could include a dependence of the transport terms (5.29), (5.31) on the 'thickness' of the basement membrane, $f(x,t)$, thereby slightly increasing the VEGF supply to the parent capillary as the basement membrane is degraded. The effect of this would be to reduce the time until the EC first escape from the parent capillary.

At the tumour side of the ECM, we need to introduce a source of VEGF, $J_v(x,t)$. We assume that there is no flux of EC, fibronectin or angiostatin and thus take the following boundary conditions:

$$\begin{aligned} -D_P \frac{\partial}{\partial y}\left(\ln\frac{P}{T}\right)(x,l,t) &= 0, && (5.32)\\ -D_V \frac{\partial V(x,l,t)}{\partial y} &= -J_v(x,t), && (5.33)\\ -D_F \frac{\partial F(x,l,t)}{\partial y} &= 0, && (5.34)\\ -D_A \frac{\partial A(x,l,t)}{\partial y} &= 0. && (5.35) \end{aligned}$$

The source function is taken to be a unimodal function, normalised so that the total flux over the boundary $y = l$ is v_0 [87]:

$$J_v(x,t) = \frac{v_0\sigma}{L}\left(1-\cos\frac{2\pi x}{L}\right)^{m_0}, \qquad (5.36)$$

where $\sigma = \left(\int_0^1 (1-\cos 2\pi x)^{m_0}\,dx\right)^{-1}$ and $v_0, m_0 \geq 0$ are constants.

We also impose no flux boundary conditions at $x = 0, L$:

$$\begin{aligned} D_P P\frac{\partial}{\partial x}\left(\ln\frac{P}{T}\right)(0,y,t) &= D_P P\frac{\partial}{\partial x}\left(\ln\frac{P}{T}\right)(L,y,t) = 0, && (5.37)\\ D_p p\frac{\partial}{\partial x}\left(\ln\frac{p}{\tau}\right)(0,t) &= D_p p\frac{\partial}{\partial x}\left(\ln\frac{p}{\tau}\right)(L,t) = 0, && (5.38)\\ D_V\frac{\partial V(0,y,t)}{\partial x} &= D_V\frac{\partial V(L,y,t)}{\partial x} = 0, && (5.39)\\ D_F\frac{\partial F(0,y,t)}{\partial x} &= D_F\frac{\partial F(L,y,t)}{\partial x} = 0, && (5.40)\\ D_A\frac{\partial A(0,y,t)}{\partial x} &= D_A\frac{\partial A(L,y,t)}{\partial x} = 0. && (5.41) \end{aligned}$$

Initially, there is a uniform distribution of EC in the capillary, and a uniform distribution of fibronectin in both the capillary and the ECM. All other quantities are zero. The initial conditions are therefore:

$$\begin{aligned} p(x,0) &= p_0, & P(x,y,0) &= 0,\\ v(x,0) &= 0, & V(x,y,0) &= 0,\\ f(x,0) &= f_0, & F(x,y,0) &= f_0,\\ c(x,0) &= 0, & C(x,y,0) &= 0,\\ a(x,0) &= 0, & A(x,y,0) &= 0, \end{aligned} \qquad (5.42)$$

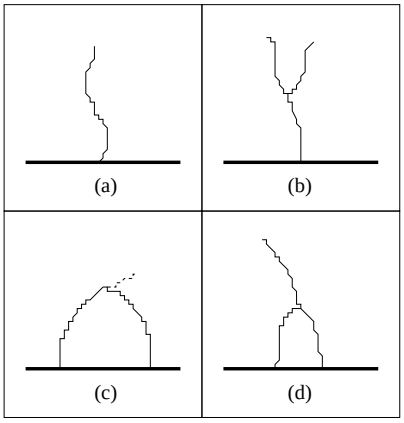

Figure 5.2: A schematic diagram of growing capillaries: (a) a migrating capillary tip. (b) a capillary branch. (c) tip-to-tip anastomosis. (d) tip-to-branch anastomosis.

Note that, for the simulations, we have taken the fibronectin concentration in the capillary (representing the thickness of the basement membrane) to be equal to that in the ECM. It is possible that the basement membrane represents a more significant obstacle for the EC than does ordinary extracellular tissue. This would suggest that f_0 should be greater in the capillary than in the ECM and the effects of this will be discussed in section 5.4.

5.1.4 Non-Dimensionalisation

Let

$$p' = \frac{p}{p_0}, \quad P' = \frac{P}{p_0}, \quad p'_m = \frac{p_m}{p_0}, \quad v' = \nu_1 v, \quad V' = \nu_1 V, \quad f' = \frac{f}{f_0}, \quad F' = \frac{F}{f_0},$$
$$c' = \nu_1 c, \quad C' = \nu_1 C, \quad a' = \nu_e a, \quad A' = \nu_e A, \quad x' = \frac{x}{L}, \quad y' = \frac{y}{L}, \quad t' = \frac{D_p}{L^2} t,$$
$$\lambda' = \frac{L^2}{h^2}.$$

The constants resulting from this scaling are rewritten in the following as K_i (see Table 5.1).

The system (5.7)–(5.11), (5.17)–(5.19) becomes (dropping the dashes):

$$\frac{\partial p_n}{\partial t} = \hat{\tau}^+_{n-1} p_{n-1} + \hat{\tau}^-_{n+1} p_{n+1} - 2\lambda p_n, \tag{5.43}$$

$$\frac{\partial v}{\partial t} = -K_1 \frac{vp}{1+v} + K_2 \left(V(x,0,t) - v(x,t) \right), \tag{5.44}$$

$$\frac{\partial c}{\partial t} = K_1 \frac{vp}{1+v} - K_3 c, \tag{5.45}$$

$$\frac{\partial f}{\partial t} = K_4 f (1-f) p - K_5 c_a f, \tag{5.46}$$

$$\frac{\partial a}{\partial t} = K_7 H\left(t - K_8\right) - K_9 a, \tag{5.47}$$

$$\hat{\tau}_n^{\pm} = \frac{2\lambda\tau\left(w_{n\pm\frac{1}{2}}\right)}{\tau\left(w_{n-\frac{1}{2}}\right) + \tau\left(w_{n+\frac{1}{2}}\right)}, \tag{5.48}$$

$$\tau\left(c_a, f, v\right) = \left(\frac{c_a + K_{10}}{c_a + K_{11}}\right)^{\gamma_1}\left(\frac{f + K_{12}}{f + K_{13}}\right)^{\gamma_2}\left(\frac{v + K_{14}}{v + K_{15}}\right)^{\gamma_3}, \tag{5.49}$$

$$c_a = \frac{c}{1 + a + K_6 f}. \tag{5.50}$$

Similarly, the ECM equations (5.12)–(5.16), (5.20)–(5.25) become:

$$\begin{aligned}\frac{\partial P_{n,m}}{\partial t} &= \hat{T}^{H+}_{n-1,m}P_{n-1,m} + \hat{T}^{H-}_{n+1,m}P_{n+1,m} + \hat{T}^{V+}_{n,m-1}P_{n,m-1} + \hat{T}^{V-}_{n,m+1}P_{n,m+1} \\ &\quad -4\lambda P_{n,m} + P_{n,m}\left[\left(K_{16} + \hat{G}\left(C_A\right)\frac{\partial C_A}{\partial t}\right) - K_{17}\right], \end{aligned}\tag{5.51}$$

$$\frac{\partial V}{\partial t} = K_{18}\nabla^2 V - K_1\frac{VP}{1+V}, \tag{5.52}$$

$$\frac{\partial C}{\partial t} = K_1\frac{VP}{1+V} - K_3 C, \tag{5.53}$$

$$\frac{\partial F}{\partial t} = K_{19}\nabla^2 F + K_{20}F\left(1 - F\right) - K_5 C_A F, \tag{5.54}$$

$$\frac{\partial A}{\partial t} = K_{21}\nabla^2 A + K_7 H\left(t - K_8\right)\left(1 - F\right) - K_9 A, \tag{5.55}$$

$$\hat{T}^{H\pm}_{n,m} = \frac{4\lambda T\left(W_{n\pm\frac{1}{2},m}\right)}{T\left(W_{n-\frac{1}{2},m}\right) + T\left(W_{n+\frac{1}{2},m}\right) + T\left(W_{n,m-\frac{1}{2}}\right) + T\left(W_{n,m+\frac{1}{2}}\right)}, \tag{5.56}$$

$$\hat{T}^{V\pm}_{n,m} = \frac{4\lambda T\left(W_{n,m\pm\frac{1}{2}}\right)}{T\left(W_{n-\frac{1}{2},m}\right) + T\left(W_{n+\frac{1}{2},m}\right) + T\left(W_{n,m-\frac{1}{2}}\right) + T\left(W_{n,m+\frac{1}{2}}\right)}, \tag{5.57}$$

$$T\left(C_A, F, V\right) = \left(\frac{C_A + K_{24}}{C_A + K_{25}}\right)^{\gamma_4}\left(\frac{F + K_{26}}{F + K_{27}}\right)^{\gamma_5}\left(\frac{V + K_{28}}{V + K_{29}}\right)^{\gamma_6}, \tag{5.58}$$

$$\hat{G}\left(C_A\right) = K_{22}\frac{e^{-K_{23}C_A^{m_1}}\left(1 - K_{23}m_1 C_A^{m_1}\right)}{1 + K_{22}C_A e^{-K_{23}C_A^{m_1}}}, \tag{5.59}$$

$$C_a = \frac{C}{1 + A + K_6 F}. \tag{5.60}$$

The boundary conditions (5.28)–(5.41) become:

$$P(x,0,t) = H\left(\frac{f_1}{f_0} - f(x,t)\right) p(x,t), \tag{5.61}$$

$$-K_{30}\frac{\partial V(x,0,t)}{\partial y} + V(x,0,t) = v(x,t), \tag{5.62}$$

$$\frac{\partial F(x,0,t)}{\partial y} = 0, \tag{5.63}$$

$$-K_{31}\frac{\partial A(x,0,t)}{\partial y} + A(x,0,t) = a(x,t), \tag{5.64}$$

$$P\frac{\partial}{\partial y}\left(\ln\frac{P}{T}\right)(x,l/L,t) = 0, \tag{5.65}$$

$$\frac{\partial V(x,l/L,t)}{\partial y} = K_{32}\left(1-\cos(2\pi x)\right)^{m_0}, \tag{5.66}$$

$$\frac{\partial F(x,l/L,t)}{\partial y} = 0, \tag{5.67}$$

$$\frac{\partial A(x,l/L,t)}{\partial y} = 0, \tag{5.68}$$

$$P\frac{\partial}{\partial x}\left(\ln\frac{P}{T}\right)(0,y,t) = P\frac{\partial}{\partial x}\left(\ln\frac{P}{T}\right)(1,y,t) = 0, \tag{5.69}$$

$$p\frac{\partial}{\partial x}\left(\ln\frac{p}{\tau}\right)(0,t) = p\frac{\partial}{\partial x}\left(\ln\frac{p}{\tau}\right)(1,t) = 0, \tag{5.70}$$

$$\frac{\partial V(0,y,t)}{\partial x} = \frac{\partial V(1,y,t)}{\partial x} = 0, \tag{5.71}$$

$$\frac{\partial F(0,y,t)}{\partial x} = \frac{\partial F(1,y,t)}{\partial x} = 0, \tag{5.72}$$

$$\frac{\partial A(0,y,t)}{\partial x} = \frac{\partial A(1,y,t)}{\partial x} = 0. \tag{5.73}$$

Finally, the initial conditions (5.42) take the form:

$$\begin{aligned} &p(x,0)=1, \quad P(x,y,0)=0,\\ &v(x,0)=0, \quad V(x,y,0)=0,\\ &f(x,0)=1, \quad F(x,y,0)=1,\\ &c(x,0)=0, \quad C(x,y,0)=0,\\ &a(x,0)=0, \quad A(x,y,0)=0. \end{aligned} \tag{5.74}$$

i	K_i	i	K_i	i	K_i	i	K_i
1	$\frac{L^2\lambda_1\delta_e p_0}{D_p}$	2	$\frac{L^2 B_1}{D_p}$	3	$\frac{L^2\mu}{D_p}$	4	$\frac{4L^2}{D_p T_f}$
5	$\frac{L^2\lambda_3}{D_p\nu_1}$	6	$f_0\nu_3$	7	$\frac{\nu_e A_r L^2}{D_p}$	8	$\frac{D_p T_{\text{iv}}}{L^2}$
9	$\frac{L^2}{D_p T_a}$	10	$\alpha_1\nu_1$	11	$\alpha_2\nu_1$	12	$\frac{\beta_1}{f_0}$
13	$\frac{\beta_2}{f_0}$	14	$\delta_1\nu_1$	15	$\delta_2\nu_1$	16	$\frac{L^2 Q}{D_p}$
17	$\frac{L^2\mu_1}{D_p}$	18	$\frac{D_V}{D_p}$	19	$\frac{D_F}{D_p}$	20	$\frac{4L^2}{D_p T_F}$
21	$\frac{D_A}{D_p}$	22	$\frac{A}{\nu_1}$	23	$\frac{\lambda_0}{\nu_1^{m_1}}$	24	$\alpha_3\nu_1$
25	$\alpha_4\nu_1$	26	$\frac{\beta_3}{f_0}$	27	$\frac{\beta_4}{f_0}$	28	$\delta_3\nu_1$
29	$\delta_4\nu_1$	30	$\frac{D_V}{L\psi}$	31	$\frac{D_A}{L\psi'}$	32	$\frac{v_0\sigma\nu_1}{D_V}$

Table 5.1: Constants resulting from the non-dimensionalisation of the model.

Length scale	$L = 0.05$ mm
EC diffusion coefficient	$D_p = D_P = 3.6 \times 10^{-6}$ mm^{2}h^{-1}
VEGF diffusion coefficient	$D_V = 3.6 \times 10^{-5}$ mm^{2}h^{-1}
Fibronectin diffusion coefficient	$D_F = 3.6 \times 10^{-10}$ mm^{2}h^{-1}
Angiostatin diffusion coefficient	$D_A = 6.5 \times 10^{-5}$ mm^{2}h^{-1}
Kinetic parameters for VEGF	$\lambda_1 = 74.8$ μM^{-1}h^{-1}
	$\nu_1 = 7.69 \times 10^{-3}$ μM^{-1}
Kinetic parameters for fibronectin	$\lambda_3 = 19.3$ μM^{-1}h^{-1}, $\nu_3 = 1.20$ μM^{-1}
Kinetic parameter for angiostatin	$\nu_e = 1$ μM^{-1}
Protease decay rate	$\mu = 4.56$ h^{-1}
Reaction times	$T_f = T_F = 18$ h, $T_a = 1$ h
Proliferation rate parameters	$Q = 8 \times 10^{-4}$ h^{-1}, $A = 44.1$ μM^{-1}
	$\lambda_0 = 1.1 \times 10^{-9}$ μM^{-2}, $m_1 = 2$
Death rate	$\mu_1 = 7.14 \times 10^{-5}$ h^{-1}
Threshold values	$f_0 = 6 \times 10^{-3}$ μM, $T_{\text{iv}} = 4.5$ h
VEGF transmission rates	$B_1 = 1.0$ h^{-1}, $\psi = 2$ mm h^{-1}
Angiostatin transmission rate	$\psi' = 2$ mm h^{-1}
VEGF source term constants	$v_0 = 0.04$ μM mm^{2}h^{-1}, $\sigma = 1.51 \times 10^{-3}$
Angiostatin source term constant	$A_r = 1700$ μM h^{-1}
Initial densities	$p_0 = 10^{-5}$ μM, $f_0 = 10^{-2}$ μM
Number of receptors per cell	$\delta_e = 10^5$
Protease TPF parameters	$\alpha_1 = 0.1$ μM, $\alpha_2 = 1.0$ μM
	$\alpha_3 = 0.1$ μM, $\alpha_4 = 1.0$ μM
Fibronectin TPF parameters	$\beta_1 = 1.0$ μM, $\beta_2 = 0.1$ μM
	$\beta_3 = 1.0$ μM, $\beta_4 = 0.5$ μM
VEGF TPF parameters	$\delta_1 = 0.1$ μM, $\delta_2 = 1.0$ μM
	$\delta_3 = 0.1$ μM, $\delta_4 = 1.0$ μM
TPF exponents	$\gamma_1 = 100$, $\gamma_2 = 100$, $\gamma_3 = 40$
	$\gamma_4 = 50$, $\gamma_5 = 37.5$, $\gamma_6 = 20$

Table 5.2: Parameter values used in the simulations.
TPF: transition probability function.

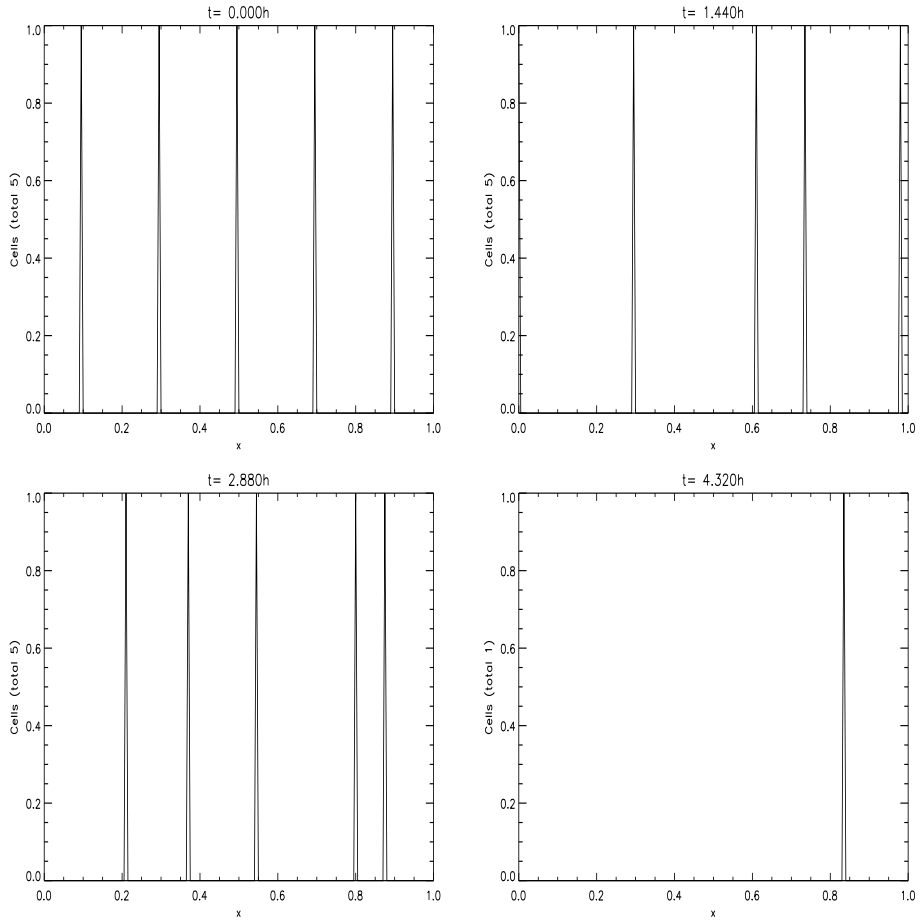

Figure 5.3: Positions of the EC in the capillary.

5.2 The Method of Simulation

Cell movement is governed by the master equations (5.43), (5.51) and the method of simulation is as described in section 3.6.

Proliferation and death are included by assuming that at any given time step, each cell has a probability $\alpha^+ (C_A, P) \geq 0$ of dividing and $\alpha^- (C_A, P) \geq 0$ of dying. Then the expected increase, in one time step, of the cell density at mesh point (n, m) is $(\alpha^+ - \alpha^-) P$. Hence by (5.51), we must have

$$\left(\alpha^+ - \alpha^-\right) P = kP \left[\left(K_{16} + \hat{G} (C_A) \frac{\partial C_A}{\partial t} \right) - K_{17} \right]. \tag{5.75}$$

Of the three terms on the right-hand side of (5.75), the background proliferation term, K_{16}, is always non-negative, the apoptosis term, $-K_{17}$, is always negative and

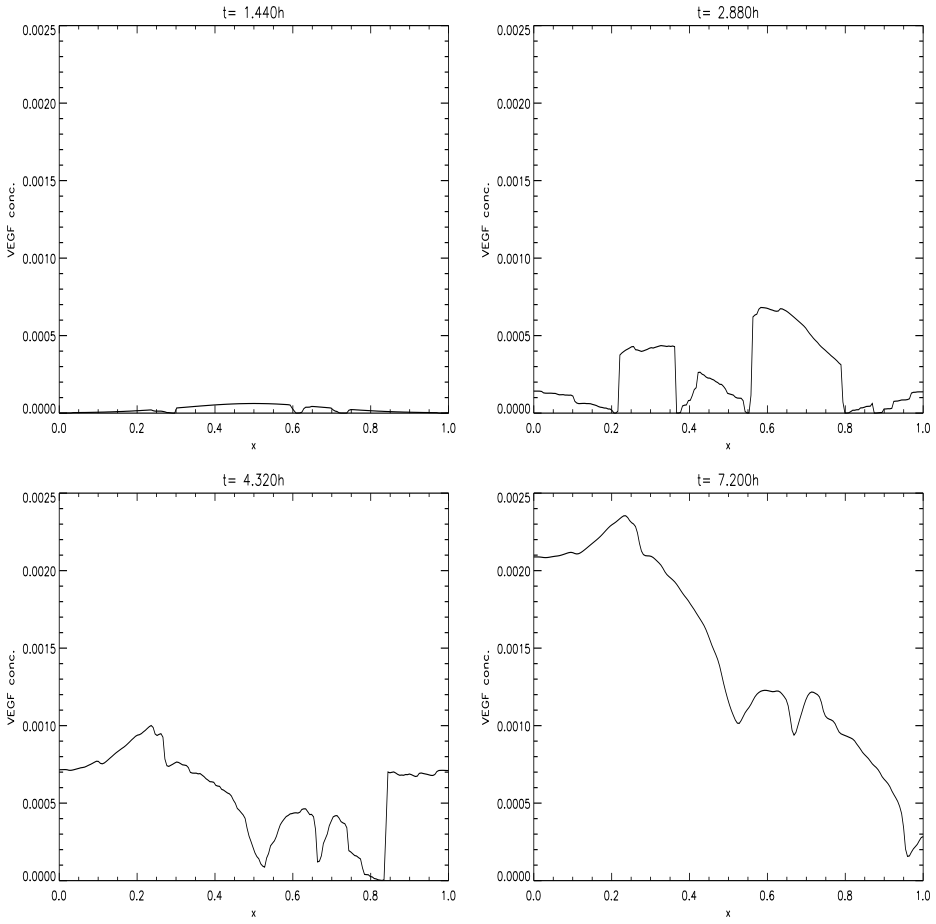

Figure 5.4: Evolution of the VEGF profile in the capillary.

the protease-dependent term, $\hat{G}(C_A)\frac{\partial C_A}{\partial t}$, can be positive or negative. We wish to satisfy (5.75) in such a way that α^+ is composed of the positive (or proliferative) terms and α^- of the negative (or death) terms.

In the case $\hat{G}(C_A)\frac{\partial C_A}{\partial t} \geq 0$, this term contributes to cell proliferation and should therefore be included in α^+. We therefore satisfy (5.75) as follows:

$$\begin{aligned} \alpha^+(C_A, P) &= kK_{16} + \hat{G}(C_A)(C_A(t) - C_A(t-k)), \\ \alpha^-(C_A, P) &= kK_{17}. \end{aligned}$$

If $\hat{G}(C_A)\frac{\partial C_A}{\partial t} < 0$, this term contributes to cell death and so needs to be included in α^-. In this case we express (5.75) as:

$$\begin{aligned} \alpha^+(C_A, P) &= kK_{16}, \\ \alpha^-(C_A, P) &= kK_{17} - \hat{G}(C_A)(C_A(t) - C_A(t-k)). \end{aligned}$$

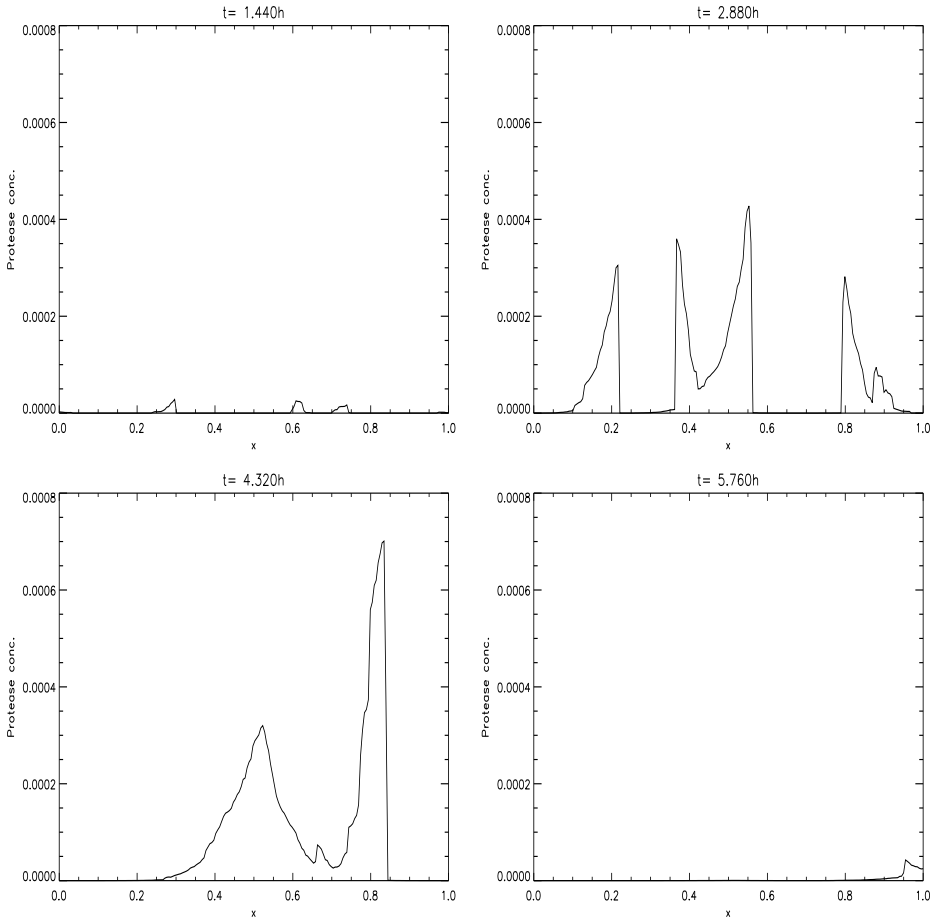

Figure 5.5: Evolution of the protease profile in the capillary.

In the capillary, cell aggregation is allowed (i.e. more than one cell is permitted to occupy a single mesh point) as this may be one mechanism by which the cells move together to degrade the capillary wall. In the ECM, however, each cell is viewed as a 'leader' cell, tracing the trajectory of a newly forming capillary tip (Figure 5.2(a)). Other EC, not included in the model, are assumed to follow the path of this leader to form the capillary lumen. When a cell divides, a new leader cell is created and the capillary branches (Figure 5.2(b)); when a cell dies, the capillary tip can move no further. When a cell collides with another cell, we have a tip-to-tip anastomosis: a closed loop is formed and only one of the capillary tips continues (Figure 5.2(c)). When a cell collides with the *trail* of another cell, we have a tip-to-branch anastomosis and the colliding capillary tip ceases to move (Figure 5.2(d)).

The differential equations (5.44)–(5.47), (5.53) are solved numerically using the Euler method. The Crank–Nicolson method is used for the PDEs (5.52), (5.54),

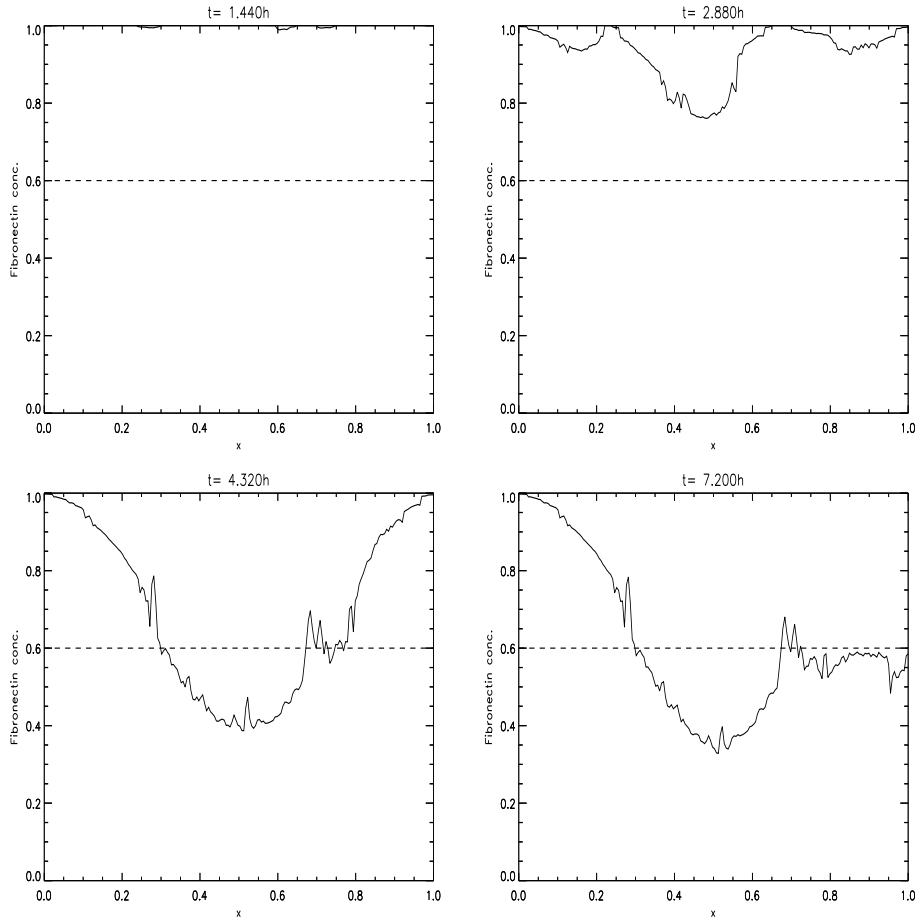

Figure 5.6: Evolution of the fibronectin profile in the capillary (the dashed line indicates the threshold level of fibronectin).

(5.55) (see appendix A).

Note that, in the computations, the cell *density* at a mesh point is calculated as being proportional to the *number* of cells at that point, with the constant of proportionality chosen so that the mean initial density in the capillary is 1. Thus if p_i and N_i are respectively the cell density and the number of cells at point i in the capillary then $p_i = \kappa N_i$ and we choose κ such that

$$\begin{aligned} \frac{1}{n}\sum_{i=1}^{n} p_i \equiv \frac{\kappa N}{n} &= 1, \\ \kappa &= \frac{n}{N}, \end{aligned}$$

where n is the number of grid points and $N = \Sigma_{i=1}^{n} N_i$ is the total number of cells.

Similarly, in the ECM we set $p_{ij} = KN_{ij}$. Note that the total mass in the capillary

is 1, so the total mass of N cells in the ECM should also be 1. We must therefore have

$$\begin{aligned} \frac{1}{n^2}\sum_{i=1}^{n}\sum_{j=1}^{n} p_{ij} \equiv \frac{KN}{n^2} &= 1, \\ K &= \frac{n^2}{N}. \end{aligned}$$

This unusual relationship between the scaling constant in the capillary and that in the ECM arises because of the coupling of a one-dimensional and a two-dimensional system via the transmission conditions, (5.26)–(5.31).

5.3 Parameter Values

The parameter values used in the simulations are shown in Table 5.2. Many of these values are taken from [87]; here we discuss the values that are particular to this model.

The substrate diffusion coefficients, D_V, D_F and D_A are taken to be a factor of 100 smaller than in [87] so that the chemotactic and haptotactic gradients that the EC detect are not destroyed. In [87] the proliferation rate, Γ, was assumed to depend on the curvature of the capillary tips. In a discrete model such as the one presented in this chapter, we are concerned with individual cells, so it does not make sense to use vessel curvature. We therefore use a constant value of Q within the range of values used in the curvature-dependent case. We use a smaller value than in [87] for the VEGF source term constant and a larger value for the angiostatin source term constant. The effects of changing the values of these parameters will be discussed in section 5.4.

We use the same parameters in the VEGF-dependent component of the transition probability function, τ_3, as in the protease-dependent component, τ_1. We use larger values for the exponents in the transition probability function than in [87] in order to elicit an adequate chemotactic response from the EC.

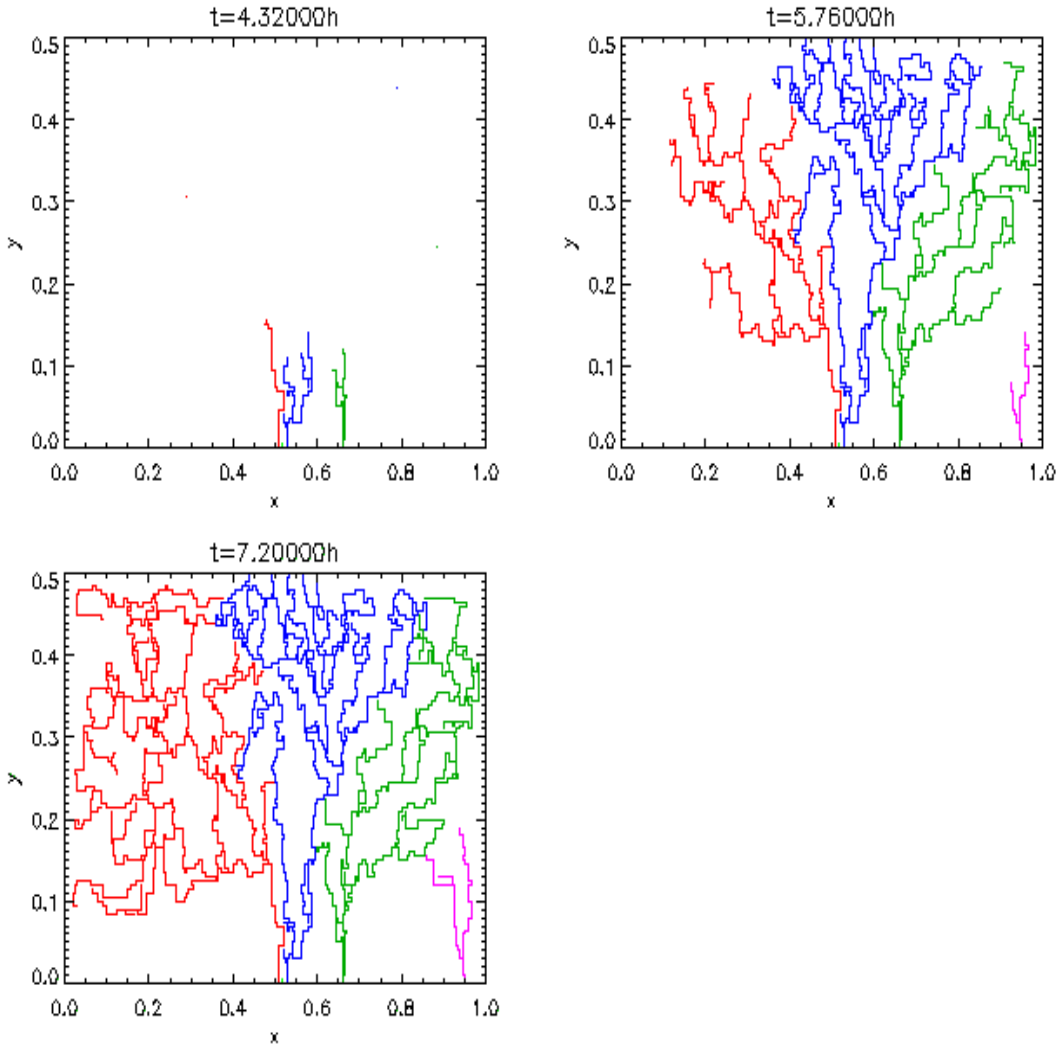

Figure 5.7: Capillary network formed by the EC in the ECM (the capillary is at $y = 0$ and the tumour is centred at $(x, y) = (0.5, 0.5)$).

5.4 Results

Simulations of the system (5.43)–(5.74) were run, together with the rules for individual cell movement and capillary branching and looping described in section 5.2. Unless stated otherwise, the parameter values are as shown in Table 5.2. The first few simulations do not include angiostatin (i.e. $A_r = 0$ in (5.27)).

Taking the average length of an EC to be 0.01 mm [87], the 0.05 mm section of capillary being modelled here will consist of approximately 5 cells. Figure 5.3 shows the positions of (the centres of) the 5 cells in the capillary at $t = 0$ h, $t = 1.44$ h,

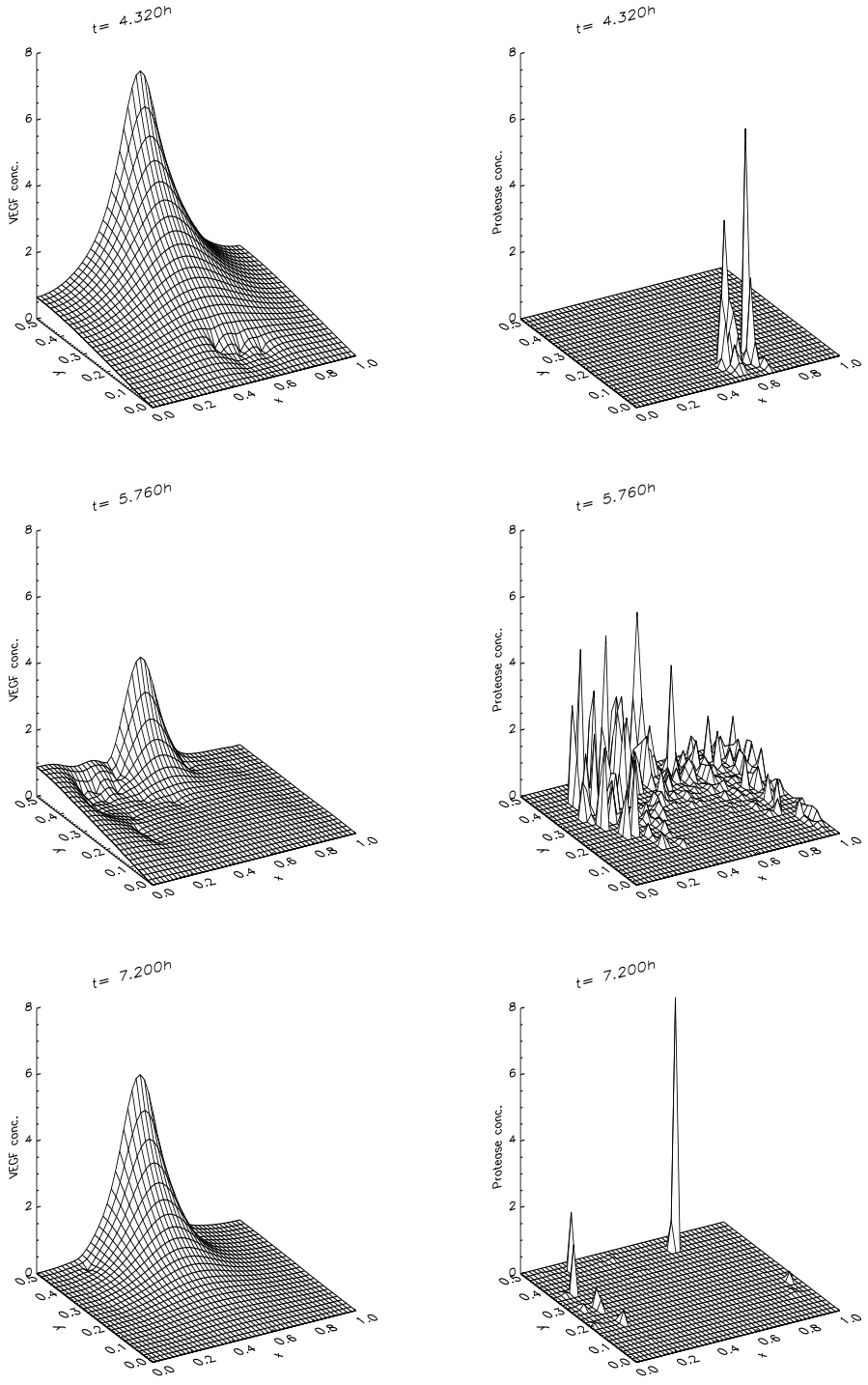

(a) (b)

Figure 5.8: Evolution of the substrate profiles in the ECM: (a) VEGF. (b) protease.

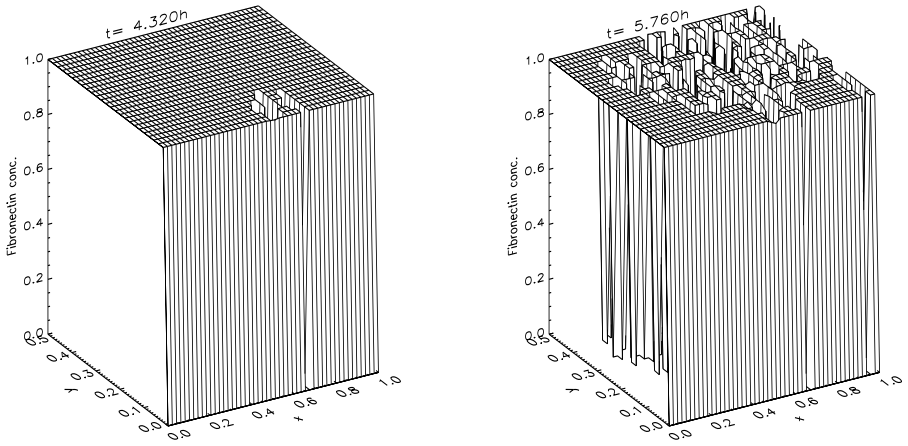

Figure 5.9: Evolution of the fibronectin profile in the ECM.

$t = 2.88$ h and $t = 4.32$ h. Figures 5.4–5.6 show how the substrate profiles evolve in the capillary. Figure 5.7 shows the trails formed by EC in the ECM and Figures 5.8 and 5.9 show how the substrates evolve in the ECM.

In Figure 5.3, the cells begin at equally spaced points along the capillary and subsequently begin to move. In Figures 5.4 and 5.5, one can see the uptake of VEGF by the EC and the resulting production of protease (at $t = 0$, there is no VEGF or protease in the capillary). The positions of the cells thus correspond to areas where VEGF has been taken up and protease has been synthesised. Figure 5.6 shows how the protease then degrades the fibronectin in the capillary wall (at $t = 0$ the fibronectin is equal to 1 everywhere). As soon as the fibronectin density falls below the threshold level of 0.6, the cells can move out of the capillary into the ECM. This first happens at $t = 4.32$ h, by which time two 'holes', (one large one between $x = 0.3$ and $x = 0.65$ and one smaller one at approximately $x = 0.75$) have been created in the fibronectin. Four of the five cells have escaped through these holes into the ECM. By the next snapshot ($t = 7.20$ h), a third hole has been made and the one remaining cell is able to escape from the capillary.

In Figure 5.7, one sees how the cells migrate across the ECM towards the tumour, forming a capillary network as they go. Recall that only the leading EC are simulated and a capillary is assumed to grow in the path of each lead cell. Note that there are only four capillaries sprouting from the parent vessel, despite the fact that five cells began the simulation. The reason for this is that two of the cells aggregated in the capillary and, when the fibronectin concentration fell below the

threshold level, were occupying the same point. They then moved into the ECM together and immediately fused, leaving just one leading cell, forming a single capillary sprout. Vessel branching is already apparent in Figure 5.7 at $t = 4.32$ h, contributing to the number of migrating capillary tips. The formation of closed capillary loops (anastomosis), which is necessary for blood flow to begin, is in evidence by $t = 5.76$ h. Also at $t = 5.76$ h, the first migrating cells have reached the tumour and angiogenesis has succeeded. Angiogenic activity continues to take place between $t = 5.76$ h and $t = 7.20$ h, resulting in a more extensive vascular network, with a greater number of capillaries making contact with the tumour. There is also some migration of EC back towards the parent vessel. This phenomenon has been observed experimentally [108], and in other mathematical models [64], and may be one mechanism responsible for the formation of closed loops.

Figure 5.8(a) shows how the VEGF is taken up by the EC as they migrate towards the tumour. Up until $t = 2.88$ h, all five cells are still in the capillary, and the VEGF profile is smooth and diffusion-dominated. At $t = 4.32$ h, there is a small number of cells in the ECM, and small irregularities are visible in the VEGF profile at the position of those cells, indicating VEGF uptake. At $t = 5.76$ h, there are many more cells in the ECM and VEGF uptake is much more pronounced, with a significant region in which all VEGF has been taken up. By $t = 7.20$ h, a diffusion-dominated profile has started to re-establish itself. This is because the bulk of the angiogenic activity has already taken place by this time: many cells have reached the tumour, and many others have formed anastomoses, and thus do not take any further part in the simulation.

Figure 5.8(b) tells a similar story with regard to the protease evolution. Again, the presence of a few cells in the ECM at $t = 4.32$ h is detectable by a few small peaks of protease. As time progresses, the number of cells increases and protease levels rise. However, by $t = 7.20$ h, protease levels have again fallen because of the decrease in the number of active cells in the ECM.

Finally, Figure 5.9 shows the path cut by the cells through the fibronectin. The cells in the ECM at $t = 4.32$ h have started to degrade fibronectin. As time passes and more capillaries start to grow, degradation becomes widespread and, by $t = 7.20$ h, the fibronectin profile has been decimated.

Note that, in the simulations, the background fibronectin level, f_0, is the same in the capillary as in the ECM. As remarked in section 5.1.3, one could choose

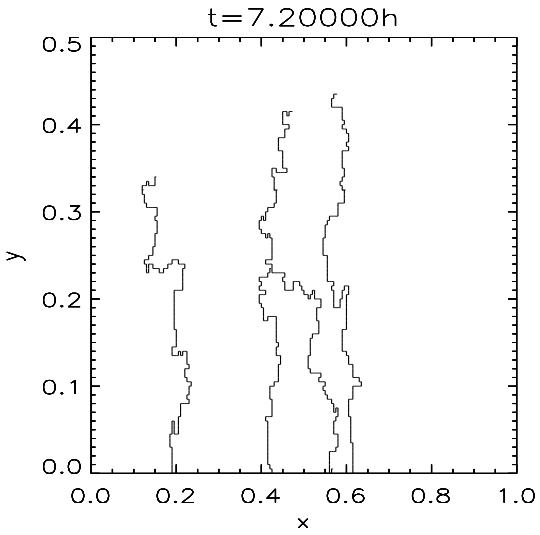

Figure 5.10: Capillary network formed in the absence of EC proliferation.

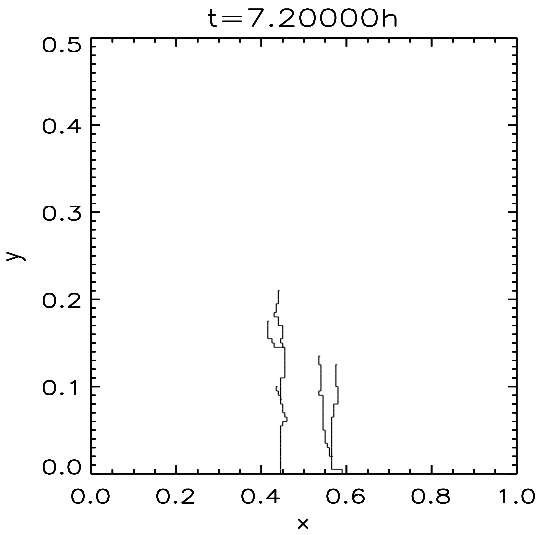

Figure 5.11: Capillary network formed with a reduced VEGF source term ($v_0 = 0.01\ \mu\text{M mm}^2\text{h}^{-1}$).

f_0 to be greater in the capillary than the ECM, representing a thicker basement membrane. Unsurprisingly, simulations run with this choice (not shown) indicate that the greater f_0 in the capillary, the longer it takes for the EC to degrade the fibronectin to the threshold level. Hence the thicker the basement membrane, the more difficult it is for EC of the parent vessel to extravasate and begin to form new vessels.

Figure 5.10 shows a simulation in which EC proliferation is not included ($\Gamma = 0$ in (5.23)). The fact that there are only four migrating capillary tips is again due to cell aggregation in the capillary prior to extravasation. In the ECM, there is, as expected, little network formation with no capillary branching and only one anastomosis. The migrating tips do not reach the tumour and vascularisation does not take place within 7.20 h. It is well known [148] that, although a primitive vascular network can form under the action of EC migration alone, proliferation is required for the formation of a fully functional network and the successful completion of angiogenesis. Thus the model is in agreement with experimental observations on this point: initial capillary sprouting occurs as normal but subsequent vascular growth is limited.

VEGF is the main regulatory factor by which tumours elicit an angiogenic response from the host [175]. To investigate further the role of VEGF, we carried out simulations with various levels of VEGF expression by the tumour. Figure 5.11 shows a simulation with a reduced VEGF source term ($v_0 = 0.01$ μM mm^{2}h^{-1} in (5.36)). This results in a greatly reduced angiogenic response, with delayed extravasation (EC did not escape the parent capillary until $t = 6.55$ h) and very little migration, branching or looping. Further reduction of the VEGF source term leads to a failure of the EC to escape the parent capillary (results not shown). These results are consistent with the fact that VEGF is the main driving force behind angiogenesis [169, 175].

Figure 5.12 shows a simulation with $v_0 = 0.2$ μM mm^{2}h^{-1} (i.e. VEGF *increased* by a factor of 5 from its standard level). As one would expect, this increases the angiogenic response. Extravasation and vascularisation take place earlier and vessel branching and looping is more pronounced, resulting in a denser capillary network.

In Figure 5.13, the source of VEGF is increased further ($v_0 = 2.0$ μM mm^{2}h^{-1}). Although the capillaries initially grow much more rapidly than in Figure 5.7, with prolific branching and looping, there is an area around the tumour in which there

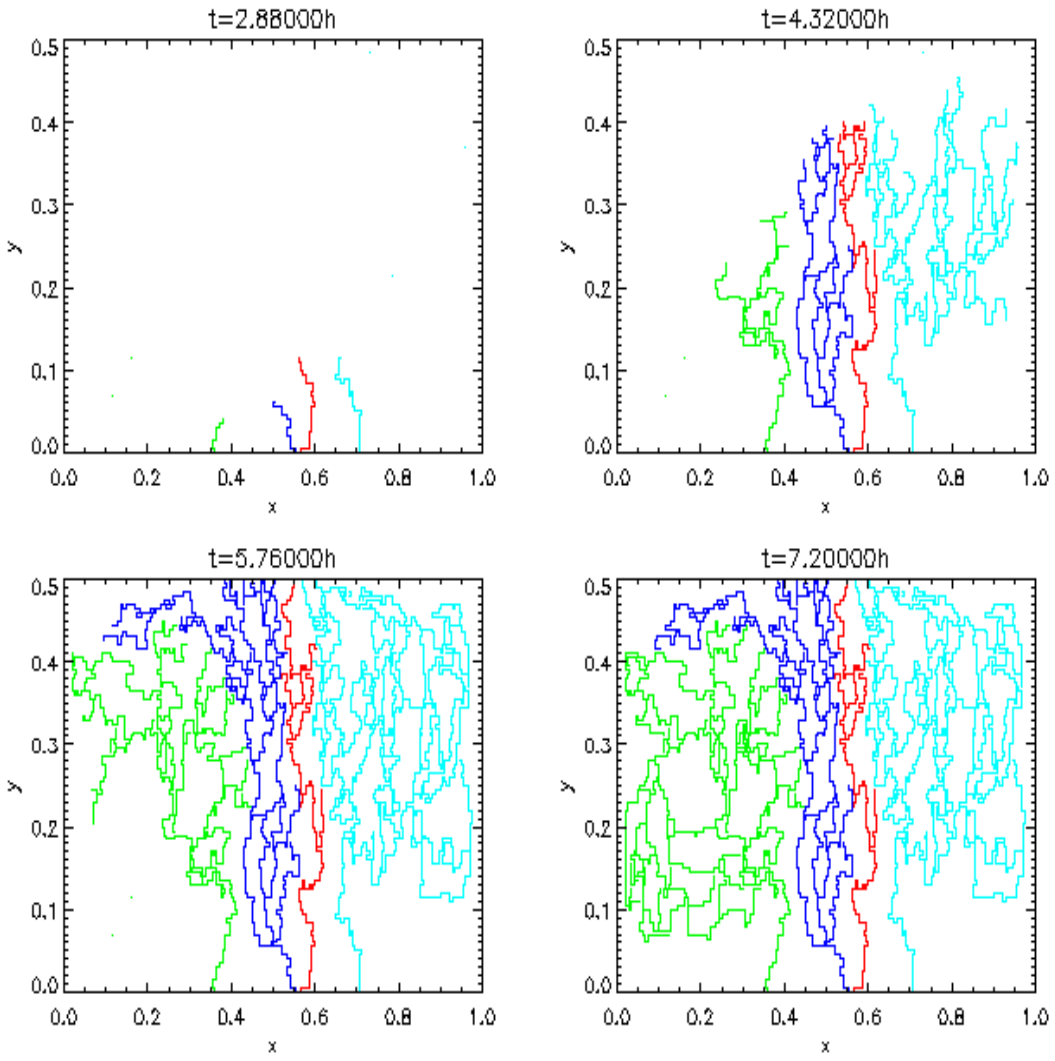

Figure 5.12: Capillary network formed with an increased VEGF source term ($v_0 = 0.2\ \mu\text{M mm}^2\text{h}^{-1}$).

is no capillary formation whatsoever: vascularisation has not taken place. There are two possible reasons for this. The first is that, as mentioned in section 5.1.2, the cells become desensitised to chemotactic gradients when the concentration of the chemoattractant is high. It is possible that the high levels of VEGF in the immediate vicinity of the tumour (see Figure 5.14) are causing a marked reduction in the chemotactic migration of the cells towards the tumour. The second reason is that the high levels of VEGF are stimulating the EC to produce large quantities of protease (see Figure 5.15). By equations (5.51), (5.59), the proliferation response of the cells initially increases with protease but subsequently peaks and falls off as the protease concentration increases further. The avascular region in Figure 5.13

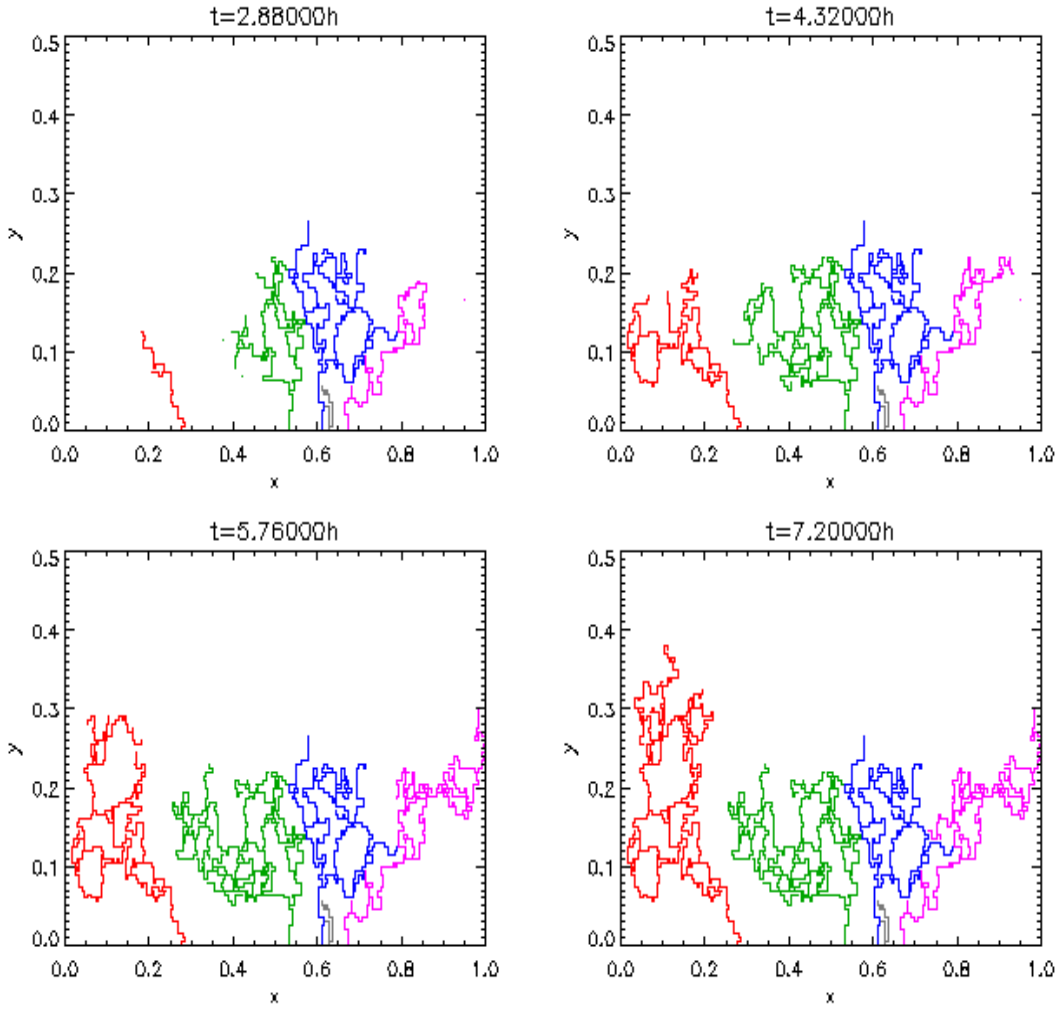

Figure 5.13: Capillary network formed with $v_0 = 2.0$ μM mm^{2}h^{-1}.

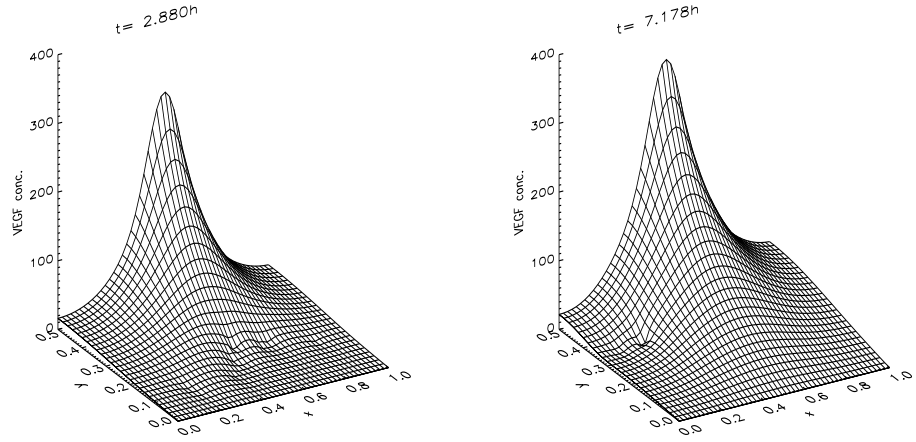

Figure 5.14: Evolution of the VEGF profile with $v_0 = 2.0$ μM mm^{2}h^{-1}.

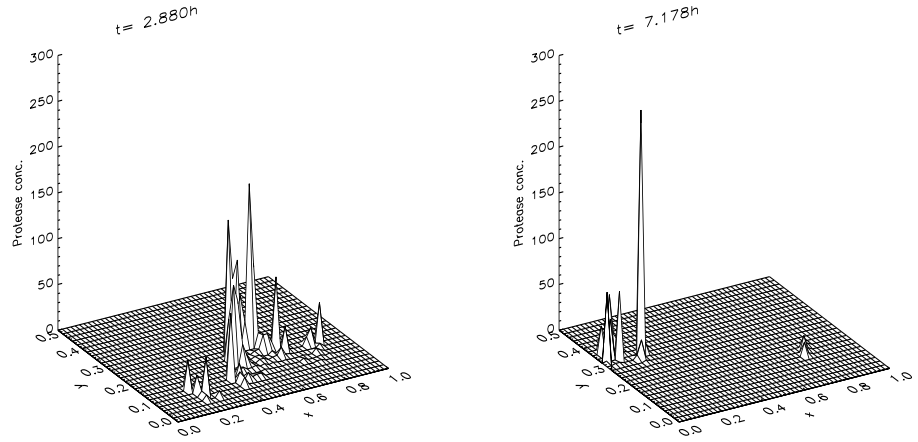

Figure 5.15: Evolution of the protease profile with $v_0 = 2.0$ μM mm^{2}h^{-1}.

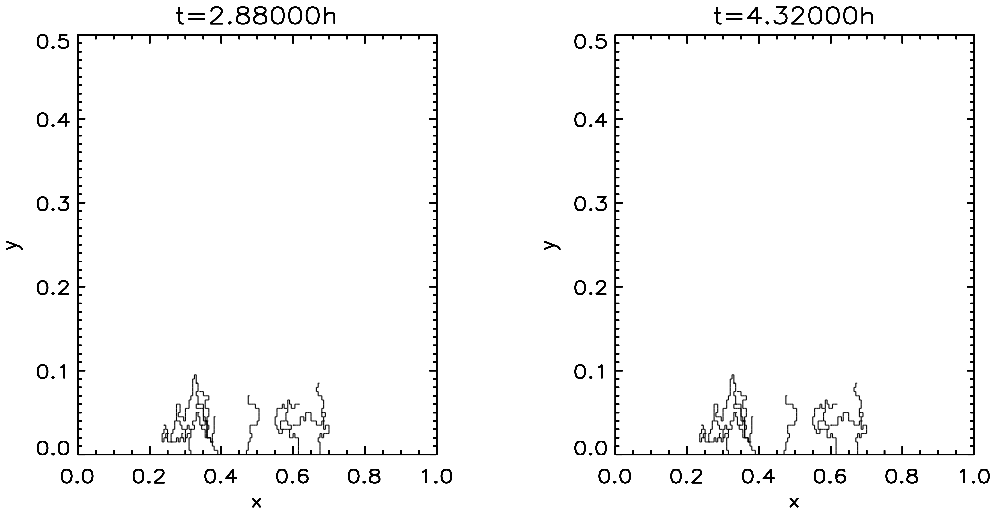

Figure 5.16: Capillary network formed with $v_0 = 40.0$ μM mm^{2}h^{-1}.

could correspond to the area where protease production is too great, leading to cell death. The most likely scenario is that it is a combination of these two factors that is causing this effect.

A phenomenon similar to this, termed the brush-border effect [109] has been observed in studies of tumour angiogenesis *in vivo*. Branching is seen to increase as the new capillaries approach the tumour, but the vessels do not initially enter the immediate vicinity of the tumour. There thus remains a narrow band of avascular tissue surrounding the tumour. This appears to be consistent with the results of this model. Moreover, we hypothesise that the reason for the brush-border effect

is that the EC encounter an excess of VEGF in the neighbourhood of the tumour. This leads to saturation of the VEGF receptors on the cell surface and the EC lose the ability to detect the VEGF gradient. It may also stimulate excess protease production, leading to cell death.

Figure 5.16 shows a simulation with $v_0 = 40$ μM mm^{2}h^{-1} (i.e. VEGF increased by a factor of 1000 from its standard level). Although the cells are very quick to escape from the parent capillary (0.92 h), there is subsequently very limited migration and the EC do not reach the tumour. By $t = 3.91$ h, all the leading EC have died and angiogenesis has stopped completely. The cells presumably enter the type of environment that existed near to the tumour in Figure 5.13 (i.e. excess VEGF resulting desensitisation to the chemotactic gradient and/or excess protease resulting in cell death) immediately on escaping from the parent vessel, thus stunting any capillary growth. The fact that cell death occurs suggests that excess protease is certainly one cause of this lack of angiogenic activity.

It has been established that the spatial and temporal expression of VEGF must be precisely regulated if angiogenesis is to succeed in forming a fully functional capillary network [55]. Deletion of the gene encoding VEGF leads to an almost complete absence of vascular development, resulting in early embryonic death [28]. Over-expression of VEGF also has adverse effects on the formation of a vascular network, causing hyperpermeability and hyperfusion [77]. This critical dependence on VEGF levels appears to be reflected in the results of this model insofar as a relatively small increase in VEGF expression can disrupt angiogenesis in the vicinity of the tumour, whereas a decrease in VEGF expression leads to inadequate EC migration and proliferation.

We now turn our attention to the potential anti-angiogenic effects of angiostatin. Recall that the effect of angiostatin in the model is to deactivate the EC-derived protease, which in turn will affect not only proteolysis of the ECM (5.54) but also EC migration (5.58) and proliferation (5.59). Figure 5.17 shows a simulation with angiostatin included. The source of angiostatin becomes active at $t = T_{\text{iv}} = 4.5$ h (5.27), so in the first snapshot, the capillaries are growing normally, under the same conditions as in Figure 5.7. However, from that point on, the angiostatin takes effect and angiogenesis proceeds at a slower rate than in Figure 5.7 and vascularisation does not take place. The uptake of VEGF (Figure 5.18) and the degradation of fibronectin (Figure 5.19) do not progress across the ECM as quickly following the

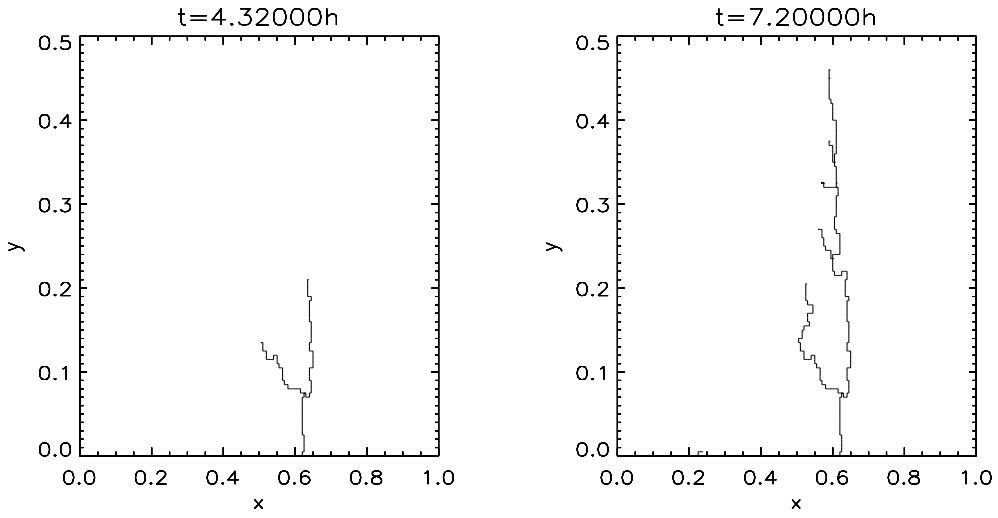

Figure 5.17: Capillary network formed when angiostatin is introduced at $t = 4.5$ h.

introduction of angiostatin. Angiostatin is supplied to the capillary uniformly (5.47) and to the ECM in areas where the fibronectin is low (5.55). The angiostatin profile (Figure 5.20) shows that the majority of the angiostatin in the ECM arrives by diffusion from the parent capillary. The function of the angiostatin is to deactivate the protease and this can be seen by comparing the total protease concentration to the active protease concentration in Figure 5.21. These are the same up to $t = 4.5$ h, but after the introduction of angiostatin, although the total protease concentration grows, active protease remains low and constitutes only a tiny proportion of total protease. By $t = 7.2$ h, almost all of the proteolytic enzyme has been deactivated by the action of the angiostatin. It is this reduction of active protease that results in a reduction of the migrating cell population, via the term $\hat{G}\left(C_A\right)\frac{\partial C_A}{\partial t}$ in (5.51), and thereby prevents the completion of angiogenesis.

Figure 5.22 shows a simulation in which angiostatin is introduced at the earlier time of $T_{\text{iv}} = 4$ h and this has successfully reduced angiogenic outgrowth still further, with very little capillary formation and no branching or looping. Supplying angiostatin immediately from $T_{\text{iv}} = 0$ h prevents extravasation of the EC (results not shown), thus stopping angiogenesis before it starts. It therefore appears that, as one would expect, the earlier angiostatin is introduced, the more effective it will be in preventing angiogenic activity. In particular, if angiostatin can be supplied to the bloodstream before EC have escaped the parent capillary, it will stand a good chance of preventing extravasation because of the dependence of this crucial event on proteolytic activity.

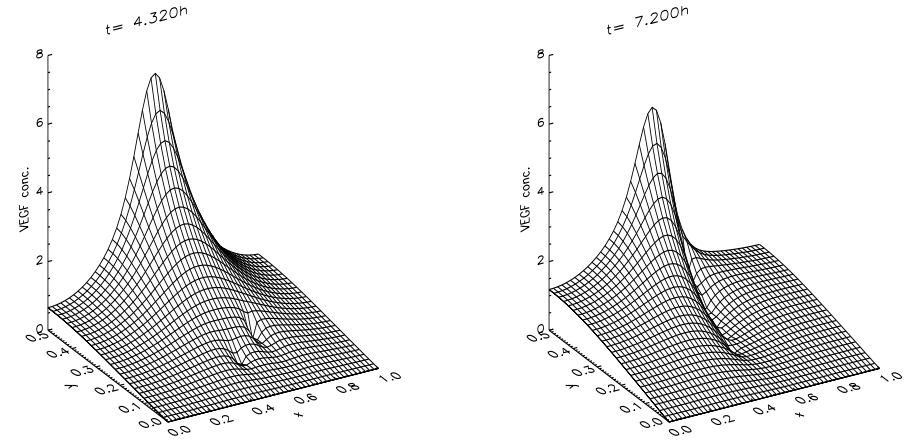

Figure 5.18: Evolution of the VEGF profile when angiostatin is introduced at $t = 4.5$ h.

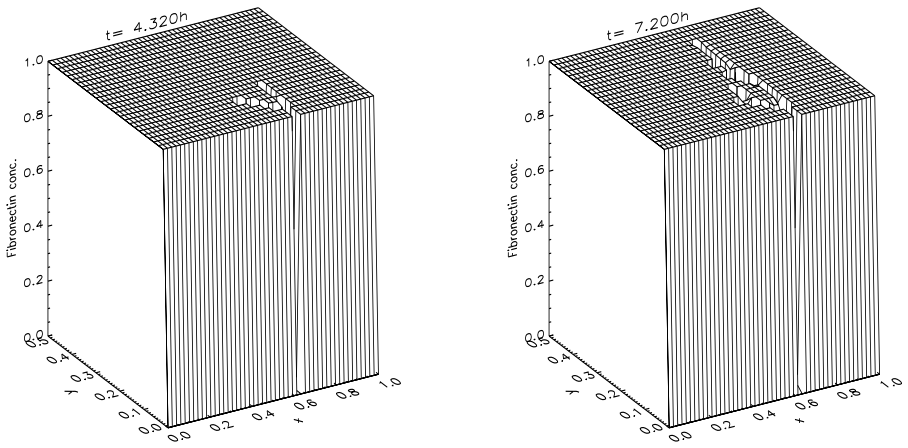

Figure 5.19: Evolution of the fibronectin when angiostatin is introduced at $t = 4.5$ h.

Administration of angiostatin is not the only anti-angiogenic therapy currently undergoing trials [25]. Another possible approach would be to prevent VEGF from activating the EC, either by directly inhibiting production of VEGF by the tumour, or via a chemical that blocks the binding of VEGF to the EC receptors [22]. To investigate the potential of this approach, we carried out a simulation in which the source of VEGF (5.66) was removed after 4.5 h, so no more VEGF enters the system after this time. Figure 5.23 shows the resulting capillary formation; Figure 5.24 shows the corresponding VEGF profiles. Although the capillaries have not quite reached the tumour after 7.2 h, they are very close to it and an advanced vascular network has formed with many closed loops allowing blood flow. Comparing this

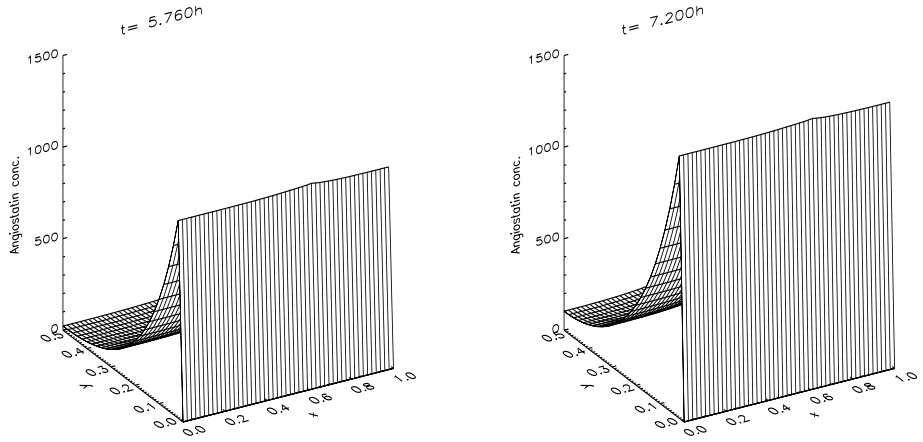

Figure 5.20: Evolution of the angiostatin profile.

with the angiostatin therapy (Figure 5.17) would therefore suggest that curtailing the supply of VEGF is not as effective an anti-angiogenic strategy as supplying angiostatin. This may be because, following the removal of the VEGF source, there is a delay while residual VEGF decays (one can see in Figure 5.24 that there is still some VEGF remaining at $t = 5.76$ h and it is not until $t = 7.20$ h that VEGF is completely removed from the system). Angiostatin, in contrast, inhibits the proteolytic enzyme as soon as it enters the system, thus having an instant impact on the angiogenic process.

This situation is analogous to the action of the angiopoietins (see section 1.5.5): Ang-1 is an agonist for the Tie-2 receptor; Ang-2 is an antagonist. The existence of such a mechanism allows the Tie-2 signalling pathway to be regulated with a high degree of spatial and temporal precision. Simply switching off expression of Ang-1 would be followed by a delay while residual ligand cleared, whereas the ability to express an antagonist, Ang-2, allows instant blocking of the Tie-2 receptor [69].

5.5 Discussion

A comparison of the results presented here with those of the continuous model of [87] (see also section 2.5.1) reveals qualitative agreement. It will be noticed, however, that the discrete modelling approach has the ability to capture features that are missed by the continuum model. In particular, a better insight can be gained

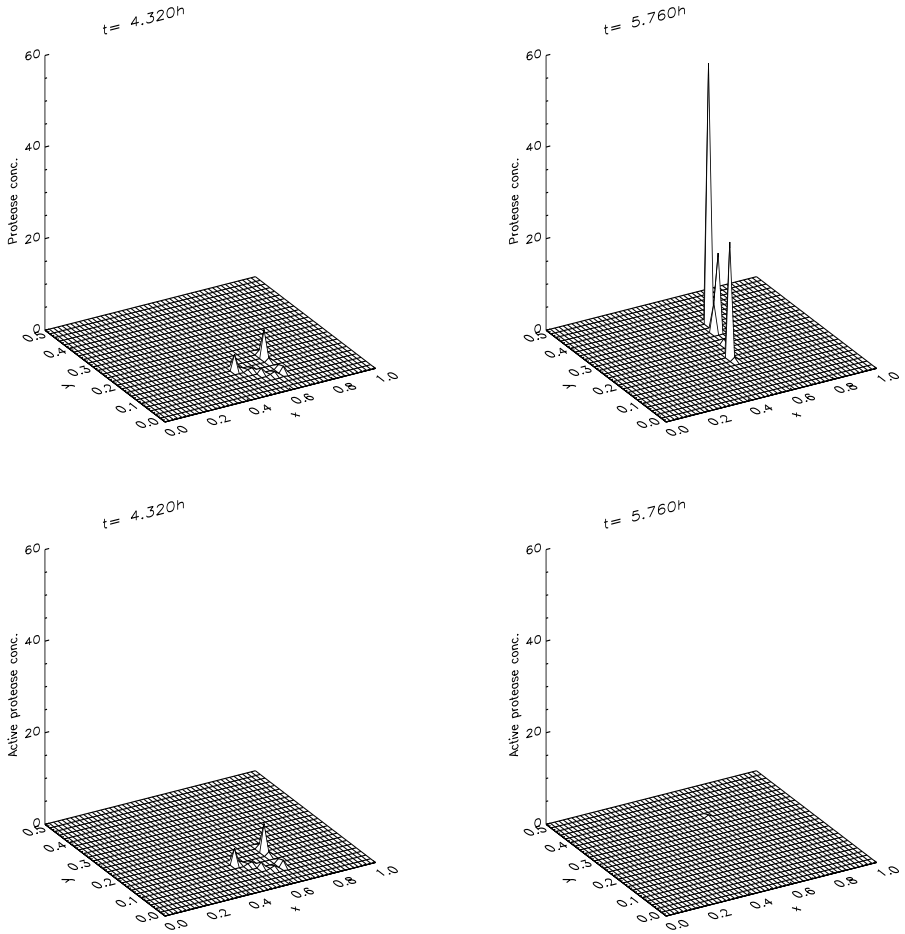

Figure 5.21: Evolution of the protease and active protease profiles when angiostatin is introduced at $t = 4.5$ h.

into the microscopic properties of the capillary network which forms in response to the tumour. The branching and looping of the vessels, processes which are not well understood biologically, can be observed directly and the effect of various factors on these processes can be studied. Furthermore, the results of this model show several important similarities with experimental observations. The early events of angiogenesis, namely EC extravasation and migration, are known to be unaffected by irradiating the EC (thus preventing proliferation), but this is incompatible with sustained angiogenic growth [148]. Our results are consistent with this. The formation of a brush-border, another phenomenon that is poorly understood, also appears to occur in our model at a certain level of VEGF production. Angiostatin, an inhibitor of angiogenesis [113], which represents a promising anti-angiogenic therapy [22], is capable of preventing vascularisation under the assumptions of the model.

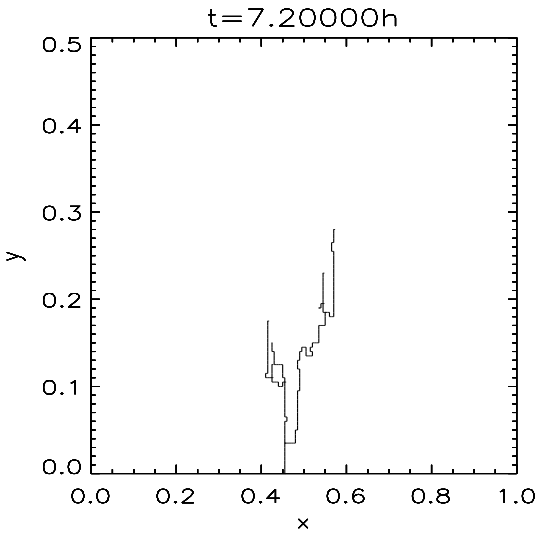

Figure 5.22: Capillary network formed when angiostatin is introduced at $t = 4$ h.

Our results suggest that, if it can be administered early enough, it would be most effective at preventing the onset of angiogenesis by blocking proteolysis of the basement membrane, which is required for EC extravasation.

This model could be extended in a number of ways. Angiogenesis is a highly complex process, involving a large number of growth factors, growth inhibitors, cell types and ECM components. The biological issues are not fully understood and there is conflicting experimental evidence regarding the roles of some of the aforementioned players. Here, we have treated the case where angiostatin acts via inhibition of protease, producing downstream effects on EC migration and proliferation. This was the hypothesis made in [153], but other mechanisms of action are possible, such as induction of EC apoptosis or a direct inhibition of EC migration.

Angiostatin is generated *in vivo* by proteolytic cleavage of plasminogen [51]. Certain tumour types may express the proteases that are required for this process [50]. Here we examined the potential anti-angiogenic effects of exogenous angiostatin administration, but tumour-mediated angiostatin generation could be easily incorporated into the model. Indeed, results (not shown) indicate that such a mechanism is capable of inhibiting angiogenesis in the neighbourhood of the tumour. It is questionable whether endogenous angiostatin would be produced in sufficient quantities to have a significant anti-angiogenic effect on the primary tumour. The effects of long range inhibition by endogenous angiostatin versus short range activation by VEGF (see

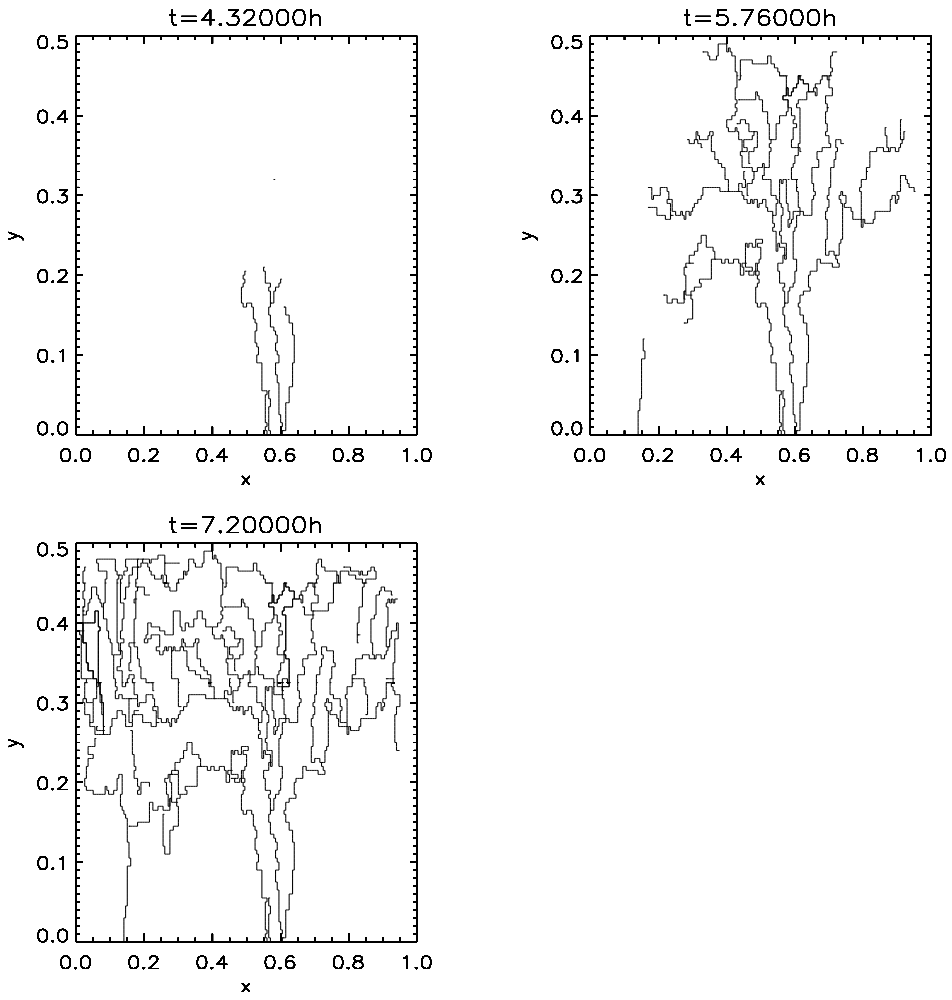

Figure 5.23: Capillary network formed when the source of VEGF is removed at $t = 4.5$ h.

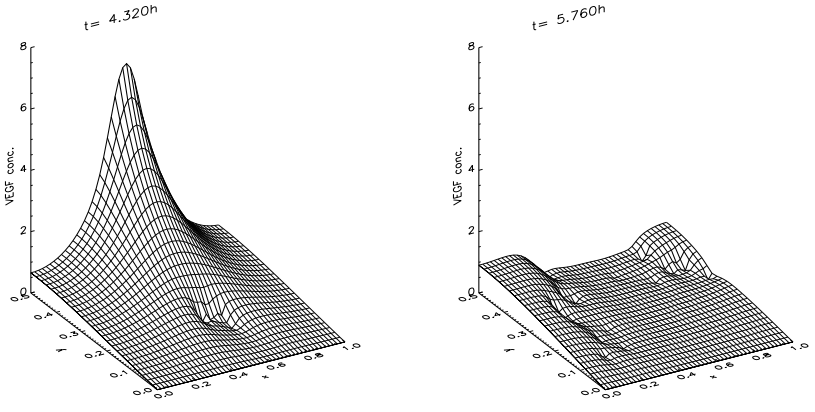

Figure 5.24: Evolution of the VEGF profile when the source of VEGF is removed at $t = 4.5$ h.

section 1.5.6) have been studied in [5], but still represent an interesting area for future research.

Another target for future work is to add to the model populations of macrophages and pericytes, which are known to play important roles in tumour angiogenesis, contributing to the production of growth factors and acting as support cells for the capillaries. A one-dimensional continuous model including macrophages and pericytes has been studied in [89] and these additional cell populations could be included in the discrete model via an appropriate master equation.

5.6 Summary

- An individual cell-based model of tumour angiogenesis, including proteolysis of the basement membrane and ECM, and the anti-angiogenic effects of angiostatin, has been constructed.
- Simulations of the model have been run, reproducing capillary networks with realistic branching and looping structures.
- Angiostatin is, under the model assumptions, capable of inhibiting angiogenesis and preventing vascularisation of the tumour.
- Key references: Levine *et al.* [87], Levine *et al.* [90], Plank and Sleeman [126].